

ARTICLE

Critical configurations of the hard-core model on square grid graphs

Simone Baldassarri^{1,2} , Vanessa Jacquier³  and Alessandro Zocca⁴ 

¹Università degli Studi di Firenze, Firenze, Italy, ²Aix-Marseille Université, Marseille, France, ³University of Utrecht, Utrecht, The Netherlands, and ⁴Vrije Universiteit Amsterdam, Amsterdam, The Netherlands

Corresponding author: Simone Baldassarri; Email: simone.baldassarri@unifi.it

(Received 14 September 2023; revised 18 December 2024; accepted 23 December 2024;
first published online: 4 February 2025)

Abstract

We consider the hard-core model on a finite square grid graph with stochastic Glauber dynamics parametrized by the inverse temperature β . We investigate how the transition between its two maximum-occupancy configurations takes place in the low-temperature regime $\beta \rightarrow \infty$ in the case of periodic boundary conditions. The hard-core constraints and the grid symmetry make the structure of the critical configurations for this transition, also known as essential saddles, very rich and complex. We provide a comprehensive geometrical characterization of these configurations that together constitute a bottleneck for the Glauber dynamics in the low-temperature limit. In particular, we develop a novel isoperimetric inequality for hard-core configurations with a fixed number of particles and show how the essential saddles are characterized not only by the number of particles but also their geometry.

Keywords: Hard-core model; metastability; tunnelling; critical configurations

2020 MSC Codes: Primary: 82C20; Secondary: 60J10, 60K35

1. Introduction

We consider a stochastic model, known in the literature as *hard-core lattice gas model* [10, 35], where particles have a non-negligible radius and therefore cannot overlap. Assuming a finite volume, the hard-core constraints are modelled with a finite undirected graph Λ . More specifically, particles can reside on the sites of Λ and edges connect the pairs of sites in Λ that cannot be occupied simultaneously. In other words, any hard-core configuration is an independent set of Λ . In this paper, we take Λ as a square grid graph with periodic boundary conditions. The resulting hard-core particle configurations are then those whose occupied sites have all the corresponding four neighbouring sites empty, see Figure 1 for an example of such configurations.

This interacting particle system evolves according to a stochastic dynamics that is fully characterized by the *Hamiltonian* or *energy function* in (2.3) and is parametrized by the *inverse temperature* β . In particular, the appearance and disappearance of particles are modelled via a Glauber-type update Markov chain $\{X_t\}_{t \in \mathbb{N}}$ with Metropolis transition probabilities induced by the Hamiltonian, see (2.4) later for more details. The stochastic process is reversible with respect to the corresponding Gibbs measure μ_β , cf. (2.2), which is then its equilibrium distribution. Specifically, for any independent set I on the graph Λ , the hard-core configuration with particles precisely on the vertices in I has stationary probability proportional to $e^{\beta|I|}$. Taking $\beta = 0$, this process can thus be used to sample uniformly independent sets of Λ .



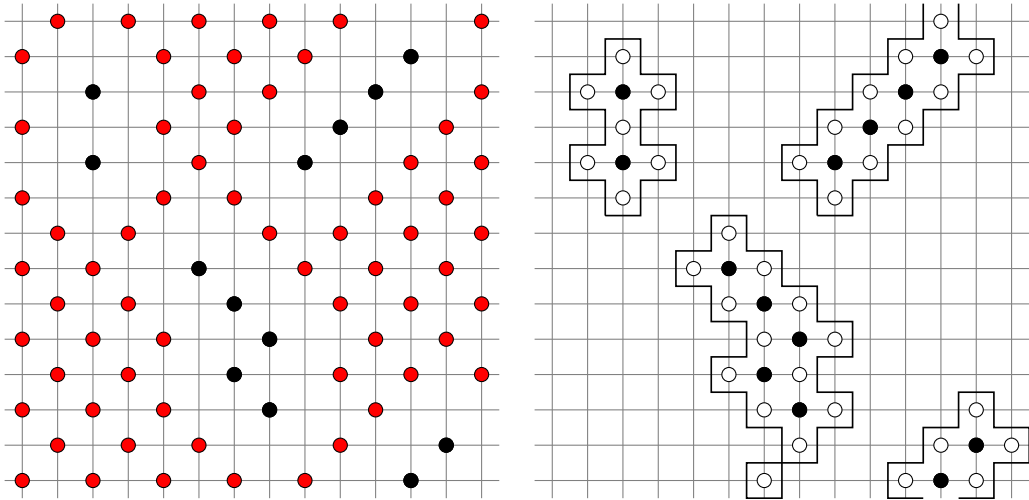


Figure 1. Example of a hard-core configuration on the 14×14 square grid with periodic boundary conditions. On the left, the occupied sites in V_o (resp. in V_e) are highlighted in black (resp. in red). On the right, we depict the same configuration using a different visual convention, in which we highlight the odd clusters that the configuration has by drawing only the empty sites in V_e (in white), the occupied sites in V_o (in black), and a black line around each odd cluster representing its contour.

Considering a regime with large β , on the other hand, the same Markov chain can also be seen as a randomized scheme with local updates to find maximum independent sets, which is an NP-hard problem [45]. Indeed, in the low-temperature regime (i.e., $\beta \rightarrow \infty$), the most likely states in view of μ_β for this interacting particle system are those with a maximum number of particles. These configurations correspond to the maximum independent sets of Λ and we will refer to them as *stable states*. On the square grid graph Λ of even length, there are two such stable states, corresponding to the two chessboard-like patterns.

When β grows large, however, it takes a very long time for the system to move from one stable state to the other, since such a transition involves visiting intermediate configurations that are very unlikely in terms of μ_β . Such transitions become thus rare events and, as a consequence, the stochastic process also takes a very long time to converge to stationarity, exhibiting so-called *slow/torpid mixing* [31, 54]. It is natural to expect such slow mixing of hard-core dynamics for a large β , since fast mixing in this regime would imply that the NP-hard problem of finding maximum independent sets could be solved or approximated efficiently.

Several papers [19, 31–33, 36, 39, 42, 44, 53] studied the slow mixing of the hard-core model by identifying how the mixing times of the Glauber dynamics scale on other graphs, depending on the type of graph, the size, the boundary conditions or the maximum vertex degree. The common main idea behind this line of work has been to identify as precisely as possible the subset of configurations that constitutes a bottleneck for the dynamics to transition from one stable state to another. Some of these approaches also heavily rely on geometric features exhibited by the configurations in this bottleneck part of the state space, like the so-called *fault lines* in [53] and *fat contours* in [36].

In this paper, we look at a complementary aspect of the hard-core model in the low-temperature regime, focusing on the hitting times between its stable states and the “bottleneck configurations” visited along these trajectories. The asymptotic behaviour of the first hitting time between the maximum-occupancy configurations of this model in the low-temperature regime $\beta \rightarrow \infty$ has already been studied in [47]. Denoting by τ_0^c the first hitting time of Markov chain $\{X_t\}_{t \in \mathbb{N}}$

corresponding to hard-core dynamics on a grid graph Λ , in [47] the authors showed that there exists a constant $\Gamma(\Lambda) > 0$ such that for every $\epsilon > 0$,

$$\lim_{\beta \rightarrow \infty} \mathbb{P}_{\beta} \left(e^{\beta(\Gamma(\Lambda) - \epsilon)} < \tau_{\mathbf{o}}^{\mathbf{e}} < e^{\beta(\Gamma(\Lambda) + \epsilon)} \right) = 1 \quad (1.1)$$

and

$$\lim_{\beta \rightarrow \infty} \frac{1}{\beta} \log \mathbb{E} \tau_{\mathbf{o}}^{\mathbf{e}} = \Gamma(\Lambda). \quad (1.2)$$

In particular, the authors showed in the same article how this constant $\Gamma(\Lambda)$, which characterizes the order of magnitude of the first hitting time between the two stable configurations, depends on the grid sizes and boundary conditions by means of an extension of the setting in [43].

However, instead of directly using the general strategy proposed in [43], which allows to jointly derive the asymptotic behaviour of the transition time as $\beta \rightarrow \infty$ together with a characterization of the critical configurations, the authors of [47] adopted a novel combinatorial method to estimate the energy barrier between the two stable states of the model, which is disentangled with respect to the description of the critical configurations. Consequently, the geometrical description of the critical configurations had yet to be addressed.

The main motivation of this paper is to fill this knowledge gap. Indeed, the geometrical characterization of the critical configurations, also known as *essential saddles*, is a relevant goal both from a probabilistic and a physical point of view since it provides insightful details of the dynamical behaviour of the system. This represents a crucial point in describing the trajectories that the system follows with high probability during the transition from one stable state to the other. We remark that in several models analysed in the context of Freidlin-Wentzell Markov chains evolving under Glauber dynamics, the *essential gate*, i.e., the set of the critical configurations, was unique [1] but, in general, there may exist many minimal sets that are crossed with high probability during the phase transition, either distinct or overlapping (see e.g., [5, 6] for this description in the case of the conservative Kawasaki dynamics). Interestingly, this is what happens also for our model despite evolving under the non-conservative Glauber dynamics. This peculiar feature relies on the hard-core constraints and on the intrinsic symmetry of the system due to the existence of two stable states. This is also the case of Glauber dynamics for the Ising and Potts models when there is no external magnetic field (see, e.g., [12]). In statistical physics, the study of such transition between stable states is usually referred to as *tunnelling*. When the particle system does not have an intrinsic symmetry or the symmetry of the system is broken, e.g., by an external magnetic field, the situation drastically changes. For interacting particle systems with a single stable state, the main object of investigation then becomes their *metastability*, i.e., the transition from the metastable state(s) to the stable one. Generally speaking, interacting particle systems that exhibit tunnelling behaviour have a much larger and complex set of essential saddles. This is precisely the case for the hard-core model on a square grid graph Λ , with the additional complication that the only admissible configurations are its independent sets.

In order to geometrically characterize the critical configurations, we associate with each cluster of particles its *contour*, that is, a union of edges on the dual graph of Λ . The equivalent representation of a configuration using its Peierls contour is a powerful tool that has been extensively used in the literature to study the phase transition of the hard-core model, identify sharper bounds for the critical temperature β_c , and to obtain high-fugacity expansion of macroscopic quantities of the model; we refer the interested reader to, e.g., [18, 38].

As part of our proof strategy, we provide some results regarding the model-dependent isoperimetric inequality for the hard-core model on grid graphs. In particular, we show that for a fixed area, the unique clusters that minimize the perimeter have a *rhomboidal* shape. However, the energy landscape is much more complex as the periodic boundary conditions give rise to other

types of clusters with minimal perimeter for a given area, such as the configurations having a column containing a fixed number of particles.

We remark that our analysis yields a comprehensive geometrical description of the configurations in the bottleneck part of the state space, together with an overview of the exact structure of the bottleneck subset itself. However, pairing this analysis with precise counting arguments is beyond the scope of the present paper. Hence, we do not explore the energy-entropy trade-off of the hard-core model or shine more light on its phase transition.

In order to link geometrical properties of hard-core configurations with the properties of the stochastic process $\{X_t\}_{t \in \mathbb{N}}$, in this paper we adopt the framework of the *pathwise approach*, introduced in the context of metastability by [24], later developed in [50, 51], and summarized in the monograph [52]. A modern version of this approach can be found in [26, 27, 43, 47]. The pathwise approach has been widely adopted for studying the low-temperature behaviour of finite-volume models with single-spin-flip Glauber dynamics, e.g., [1, 2, 11–14, 25, 49, 55, 56], with Kawasaki dynamics, e.g., [4–7, 37, 46], and with parallel dynamics, e.g., [28–30]. The more involved infinite-volume limit at low temperature was studied via this approach in [3, 34, 37]. A different method to study the limiting behaviour of interacting particle systems is the so-called *potential-theoretic approach*, initiated in [22] and later summarized in the monograph [23] (see, for instance, [20, 21, 48] for the application of this approach to specific models both in finite and infinite volume). Since these two approaches rely on different definitions of metastable states, they are not completely equivalent. The situation is particularly delicate for infinite-volume systems, irreversible systems, and degenerate systems, as discussed in [15, 26, 27]. More recent approaches are developed in [8, 9, 16, 17, 40, 41].

The paper is organized as follows. In section 2, we provide a detailed model description and state our main result regarding the geometric features of the critical configurations, Theorem 2.1. The rest of the paper is then devoted to the proof of this result. First, section 3 provides some preliminary definitions and auxiliary results, and then finally the proof of the main theorem is given in section 4. For the sake of clarity, the proofs of some auxiliary lemmas are deferred to a later section, namely section 5. Lastly, section 6 concludes the paper and discusses some future work.

2. Model description and main results

We consider the stochastic evolution of the hard-core model on finite two-dimensional square lattices. More precisely, given an integer $L \geq 2$ we consider the $L \times L$ square grid graph $\Lambda = (V, E)$ with periodic boundary conditions, which we will refer to as $L \times L$ *toric grid graph*. We denote by E the edge set of the grid graph Λ and by V the collection of its $N = L^2$ sites. We identify each site $v \in \Lambda$ by its coordinates (v_1, v_2) , that is, we take $V := \{0, \dots, L-1\} \times \{0, \dots, L-1\}$ as set of sites. In the rest of the paper, we will assume that L is an even integer, which guarantees that Λ is a bipartite graph, and that $L \geq 6$, to avoid pathological trivial cases.

A particle configuration on Λ is described by associating a variable $\sigma(v) \in \{0, 1\}$ with each site $v \in \Lambda$, indicating the absence (0) or the presence (1) of a particle on that site. Let $\mathcal{X} \subset \{0, 1\}^N$ be the collection of *hard-core configurations* on Λ , i.e.,

$$\mathcal{X} := \{\sigma \in \{0, 1\}^N \mid \sigma(v)\sigma(w) = 0, \forall (v, w) \in E\}, \quad (2.1)$$

i.e., the particle configurations on Λ with no particles residing on neighbouring sites.

A site of Λ is called *even* (respectively *odd*) if the sum of its two coordinates is even (respectively odd) and we denote by V_e and V_o the collection of even sites and that of odd sites of Λ . Clearly $|V_e| = |V_o| = L^2/2$. We denote by \mathbf{e} (\mathbf{o} , respectively) the particle configuration on Λ with particles at each site in V_e (V_o , respectively), i.e.,

$$\mathbf{e}(v) := \begin{cases} 1 & \text{if } v \in V_e, \\ 0 & \text{if } v \in V_o, \end{cases} \quad \text{and} \quad \mathbf{o}(v) := \begin{cases} 0 & \text{if } v \in V_e, \\ 1 & \text{if } v \in V_o. \end{cases}$$

Both \mathbf{e} and \mathbf{o} are hard-core configurations due to the assumption that L is even.

Figure 1 shows an example of a hard-core configuration. Throughout the paper, all figures are drawn using the following conventions. They all depict hard-core configurations on a 14×14 grid with periodic boundary conditions. The occupied (empty) sites in V_e (V_o , respectively) are shown in black (white), and we draw a black line around each odd cluster representing its contour. We tacitly assume that all the even (odd) sites outside the odd region are occupied (empty, respectively) but they are not displayed to avoid cluttering the figures. See subsection 3.1 for more precise definitions of odd clusters and odd regions.

Consider the Gibbs measure on \mathcal{X} given by

$$\mu_\beta(\sigma) := \frac{e^{-\beta H(\sigma)}}{Z_{\beta, \Lambda}}, \quad \sigma \in \mathcal{X}, \tag{2.2}$$

where H is the Hamiltonian $H : \mathcal{X} \rightarrow \mathbb{R}$ that is taken to be proportional to the number of present particles, namely

$$H(\sigma) := - \sum_{v \in V} \sigma(v), \tag{2.3}$$

with $Z_{\beta, \Lambda} := \sum_{\sigma \in \mathcal{X}} e^{-\beta H(\sigma)}$ being the normalizing constant. The two hard-core configurations on the $L \times L$ toric grid graph Λ introduced above have energy equal to

$$H(\mathbf{e}) = H(\mathbf{o}) = -\frac{L^2}{2},$$

which is the minimum value the Hamiltonian can take on \mathcal{X} [47].

We assume the interacting particle system described evolves according to stochastic Glauber-type dynamics described by a single-step update Markov chain $\{X_t^\beta\}_{t \in \mathbb{N}}$ on \mathcal{X} with transition probabilities between any pair of configurations $\sigma, \sigma' \in \mathcal{X}$ given by

$$P_\beta(\sigma, \sigma') := \begin{cases} q(\sigma, \sigma') e^{-\beta[H(\sigma') - H(\sigma)]^+}, & \text{if } \sigma \neq \sigma', \\ 1 - \sum_{\eta \neq \sigma} P_\beta(\sigma, \eta), & \text{if } \sigma = \sigma', \end{cases} \tag{2.4}$$

where $[\cdot]^+ = \max\{\cdot, 0\}$ and q is the *connectivity matrix* that allows only single-step updates, i.e., for every $\sigma, \sigma' \in \mathcal{X}$ we set

$$q(\sigma, \sigma') := \begin{cases} \frac{1}{N}, & \text{if } |\{v \in V : \sigma(v) \neq \sigma'(v)\}| = 1, \\ 0, & \text{if } |\{v \in V : \sigma(v) \neq \sigma'(v)\}| > 1. \\ 1 - \sum_{\eta \neq \sigma} q(\sigma, \eta), & \text{if } \sigma = \sigma'. \end{cases} \tag{2.5}$$

The resulting dynamics P_β is reversible with respect to the Gibbs measure μ_β given in (2.2). The triplet (\mathcal{X}, H, q) is usually referred to as *energy landscape* and (2.4) as *Metropolis transition probabilities*.

The connectivity matrix q given in (2.5) is irreducible, i.e., for any pair of configurations $\sigma, \sigma' \in \mathcal{X}$, $\sigma \neq \sigma'$, there exists a finite sequence ω of configurations $\omega_1, \dots, \omega_n \in \mathcal{X}$ such that $\omega_1 = \sigma$, $\omega_n = \sigma'$ and $q(\omega_i, \omega_{i+1}) > 0$, for $i = 1, \dots, n - 1$. We will refer to such a sequence as a *path* from σ to σ' and denote it by $\omega : \sigma \rightarrow \sigma'$. Given a path $\omega = (\omega_1, \dots, \omega_n)$, we define its *height* Φ_ω as

$$\Phi_\omega := \max_{i=1, \dots, n} H(\omega_i). \tag{2.6}$$

The *communication energy* between two configurations $\sigma, \sigma' \in \mathcal{X}$ is the minimum value that has to be reached by the energy in every path $\omega : \sigma \rightarrow \sigma'$, i.e.,

$$\Phi(\sigma, \sigma') := \min_{\omega: \sigma \rightarrow \sigma'} \Phi_\omega = \min_{\omega: \sigma \rightarrow \sigma'} \max_{\eta \in \omega} H(\eta). \tag{2.7}$$

Let $\mathcal{X}^s \subset \mathcal{X}$ denote the set of global minima of the Hamiltonian H on \mathcal{X} , to which we will refer to as *stable states*.

In [47] it has been proved that for the hard-core model on a finite $L \times L$ square grid graph the following statements hold:

- (i) There are exactly two stable states

$$\mathcal{X}^s = \{\mathbf{e}, \mathbf{o}\}; \tag{2.8}$$

- (ii) The communication energy between the two stable states is equal to

$$\Phi(\mathbf{e}, \mathbf{o}) - H(\mathbf{e}) = L + 1; \tag{2.9}$$

- (iii) The corresponding energy landscape has no deep wells, i.e.,

$$\max_{\sigma \in \mathcal{X}} [\Phi(\sigma, \{\mathbf{e}, \mathbf{o}\}) - H(\sigma)] \leq L < \Phi(\mathbf{e}, \mathbf{o}) - H(\mathbf{e}). \tag{2.10}$$

Together, these facts imply that the value of the constant appearing in the asymptotic statements (1.1) and (1.2) for the first hitting time τ_0^e is $\Gamma(\Lambda) = L + 1$.

2.1 Essential saddle characterization

Our results give insight into the way the transitions between \mathbf{e} and \mathbf{o} most likely occur in the low-temperature regime. This is usually described by identifying the optimal paths, saddles, and essential saddles that we define as follows.

- $\mathcal{S}(\mathbf{e}, \mathbf{o})$ is the *communication level set* between \mathbf{e} and \mathbf{o} defined by

$$\mathcal{S}(\mathbf{e}, \mathbf{o}) := \{\sigma \in \mathcal{X} \mid \exists \omega \in (\mathbf{e} \rightarrow \mathbf{o})_{\text{opt}}, : \sigma \in \omega \text{ and } H(\sigma) = \Phi_\omega = \Phi(\mathbf{e}, \mathbf{o})\},$$

where $(\mathbf{e} \rightarrow \mathbf{o})_{\text{opt}}$ is the set of *optimal paths* from \mathbf{e} to \mathbf{o} realizing the minimax in $\Phi(\mathbf{e}, \mathbf{o})$, i.e.,

$$(\mathbf{e} \rightarrow \mathbf{o})_{\text{opt}} := \{\omega : \mathbf{e} \rightarrow \mathbf{o} \mid \Phi_\omega = \Phi(\mathbf{e}, \mathbf{o})\}.$$

- The configurations in $\mathcal{S}(\mathbf{e}, \mathbf{o})$ are called *saddles*. Given an optimal path $\omega \in (\mathbf{e} \rightarrow \mathbf{o})_{\text{opt}}$, we define the set of its saddles $S(\omega)$ as $S(\omega) := \{\sigma \in \omega \mid H(\sigma) = \Phi_\omega = \Phi(\mathbf{e}, \mathbf{o})\}$. A saddle $\sigma \in \mathcal{S}(\mathbf{e}, \mathbf{o})$ is called *essential* if either

- (i) $\exists \omega \in (\mathbf{e} \rightarrow \mathbf{o})_{\text{opt}}$ such that $S(\omega) = \{\sigma\}$, or
- (ii) $\exists \omega \in (\mathbf{e} \rightarrow \mathbf{o})_{\text{opt}}$ such that $\sigma \in S(\omega)$ and $S(\omega') \not\subseteq S(\omega) \setminus \{\sigma\} \quad \forall \omega' \in (\mathbf{e} \rightarrow \mathbf{o})_{\text{opt}}$.
A saddle $\sigma \in \mathcal{S}(\mathbf{e}, \mathbf{o})$ that is not essential is called *unessential saddle* or *dead-end*, i.e., for any $\omega \in (\mathbf{e} \rightarrow \mathbf{o})_{\text{opt}}$ such that $\omega \cap \{\sigma\} \neq \emptyset$ we have that $S(\omega) \setminus \{\sigma\} \neq \emptyset$ and there exists $\omega' \in (\mathbf{e} \rightarrow \mathbf{o})_{\text{opt}}$ such that $S(\omega') \subseteq S(\omega) \setminus \{\sigma\}$.

- The *essential gate* $\mathcal{G}(\mathbf{e}, \mathbf{o}) \subset \mathcal{X}$ is the collection of essential saddles for the transition $\mathbf{e} \rightarrow \mathbf{o}$.

The aim of the present paper is to accurately identify the set $\mathcal{G}(\mathbf{e}, \mathbf{o})$ of essential saddles for the transition from \mathbf{e} to \mathbf{o} for the Metropolis dynamics of the hard-core model on a $L \times L$ grid with periodic boundary conditions.

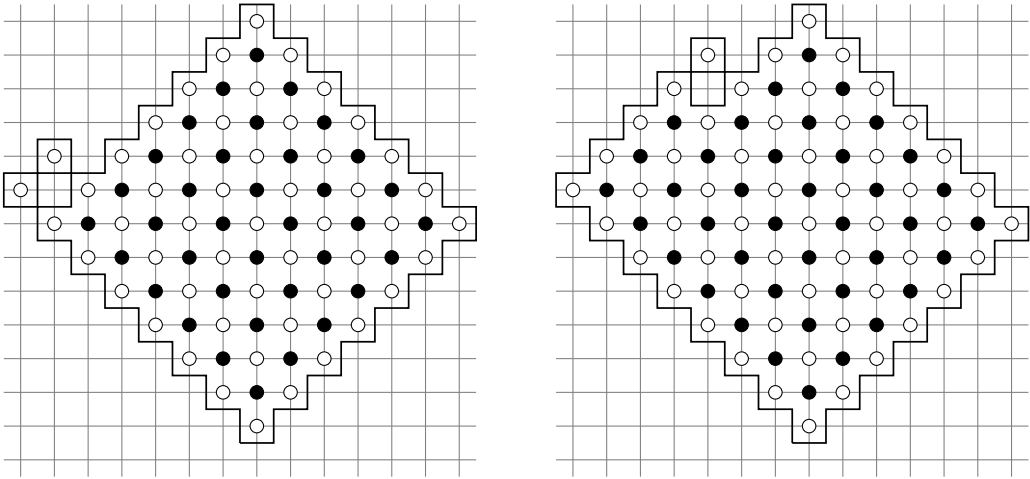


Figure 2. An example of a configuration in $C_{ir}(\mathbf{e}, \mathbf{o})$ (on the left) and one in $C_{gr}(\mathbf{e}, \mathbf{o})$ (on the right).

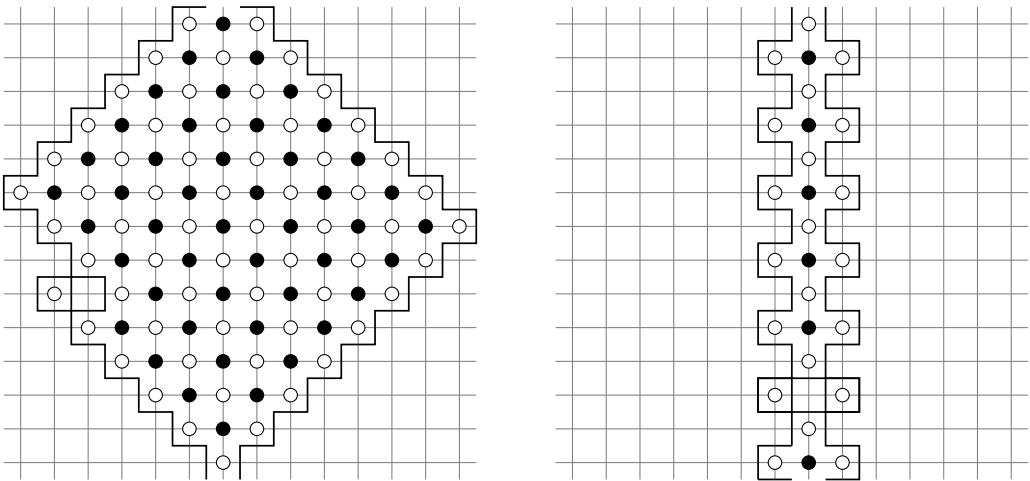


Figure 3. An example of a configuration in $C_{cr}(\mathbf{e}, \mathbf{o})$ (on the left) and one in $C_{sb}(\mathbf{e}, \mathbf{o})$ (on the right).

The set $\mathcal{G}(\mathbf{e}, \mathbf{o})$ will be described as the union of six disjoint sets, each characterized by configurations with specific geometrical features. Although we refer the reader to section 4 for a precise definition of these sets (cf. Definitions 4.2–4.6), we provide here some intuitive descriptions of the geometrical features of the configurations in these sets. We denote by

- $C_{ir}(\mathbf{e}, \mathbf{o})$, $C_{gr}(\mathbf{e}, \mathbf{o})$, and $C_{cr}(\mathbf{e}, \mathbf{o})$ the collections of configurations with a unique cluster of particles in odd sites of rhomboidal shape with exactly two adjacent even empty sites as in Figure 2 and Figure 3 (left). Roughly speaking, $C_{ir}(\mathbf{e}, \mathbf{o})$ contains the configurations with $(\frac{L}{2} - 1)^2$ occupied odd particles and $L^2 + 2$ empty even sites; $C_{gr}(\mathbf{e}, \mathbf{o})$ (resp. $C_{cr}(\mathbf{e}, \mathbf{o})$) contains the configurations obtained from $C_{ir}(\mathbf{e}, \mathbf{o})$ (resp. $C_{gr}(\mathbf{e}, \mathbf{o})$) by removing some occupied even sites attached to the rhombus and growing along one (resp. the longest) side by adding some particles in the nearest odd sites of the rhombus.

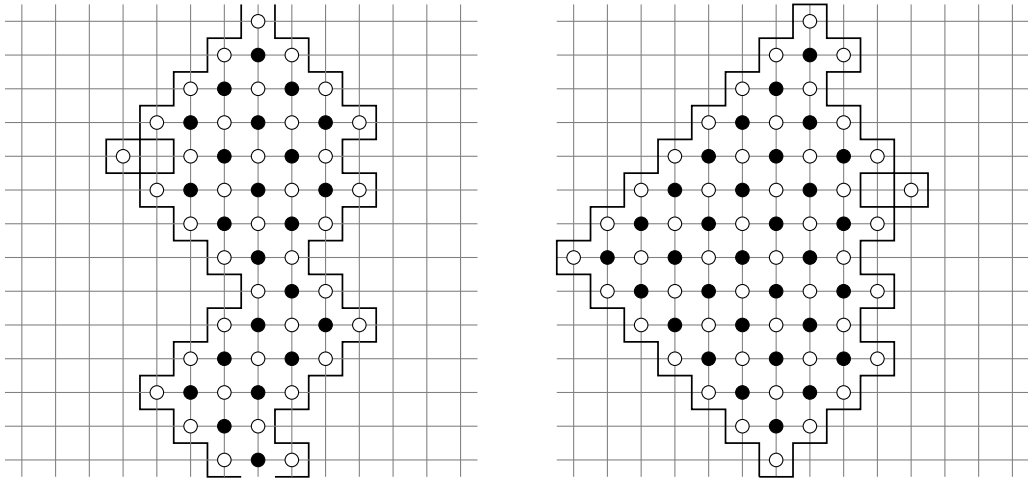


Figure 4. An example of a configuration in $C_{mb}(\mathbf{e}, \mathbf{o})$ (on the left) and one in $C_{ib}(\mathbf{e}, \mathbf{o})$ (on the right).

- $C_{sb}(\mathbf{e}, \mathbf{o})$, $C_{mb}(\mathbf{e}, \mathbf{o})$, and $C_{ib}(\mathbf{e}, \mathbf{o})$ the collections of configurations with a unique cluster of particles at odd sites with at most two additional empty even sites as in Figure 3 (right) and in Figure 4. In particular, $C_{sb}(\mathbf{e}, \mathbf{o})$ contains the configurations with $\frac{L}{2} - 1$ particles arranged in an odd column with two other empty even sites; $C_{mb}(\mathbf{e}, \mathbf{o})$ contains the configurations obtained from $C_{sb}(\mathbf{e}, \mathbf{o})$ such that there is at least one column or row with $\frac{L}{2}$ particles arranged in odd sites. $C_{ib}(\mathbf{e}, \mathbf{o})$ contains the configurations obtained from $C_{sb}(\mathbf{e}, \mathbf{o})$ without having column or row with $\frac{L}{2}$ particles.

The following theorem characterizes the essential gate for the transition from \mathbf{e} to \mathbf{o} .

Theorem 2.1 (Essential saddles). *Define the set*

$$C^*(\mathbf{e}, \mathbf{o}) := C_{ir}(\mathbf{e}, \mathbf{o}) \cup C_{gr}(\mathbf{e}, \mathbf{o}) \cup C_{cr}(\mathbf{e}, \mathbf{o}) \cup C_{sb}(\mathbf{e}, \mathbf{o}) \cup C_{mb}(\mathbf{e}, \mathbf{o}) \cup C_{ib}(\mathbf{e}, \mathbf{o}).$$

The essential saddles for the transition from \mathbf{e} to \mathbf{o} of the hard-core model on a $L \times L$ toric grid graph Λ are all and only the configurations in $C^(\mathbf{e}, \mathbf{o})$, i.e.,*

$$\mathcal{G}(\mathbf{e}, \mathbf{o}) = C^*(\mathbf{e}, \mathbf{o}).$$

Furthermore, the possible transitions at energy not higher than $-\frac{L^2}{2} + L + 1$ among the six subsets that form $C^(\mathbf{e}, \mathbf{o})$ are as detailed in Figure 5.*

3. Definitions and auxiliary results

The main goal of this section is to introduce the notion of odd clusters, which are the basis of the geometrical description of the configurations, and to inspect the relation between their shape and perimeter.

In subsection 3.1 we define a geometrical representation of clusters associated with the occupied odd sites, and in subsection 3.2 we introduce the notion of rhombi, which turns out to be crucial in the description of the essential saddles. In subsection 3.3 we present two algorithms that, combined together, return a path whose last configuration has a rhomboidal shape and such that the energy along it never increases. We will use them to deduce that there exists a downhill path from the configurations without a rhomboidal cluster towards \mathbf{e} or \mathbf{o} .

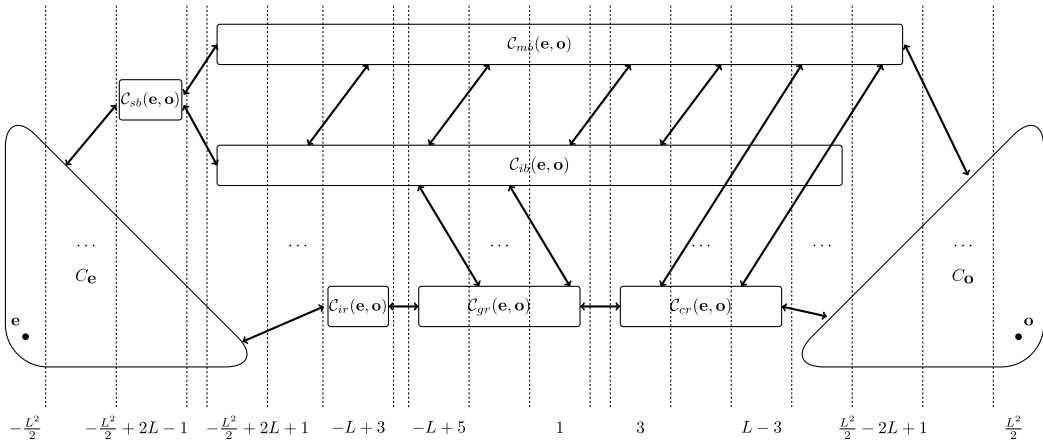


Figure 5. Schematic representation of the set of essential saddles, where we highlight with arrows between the set pairs that communicate at energy not higher than $-\frac{L^2}{2} + L + 1$ and the initial cycles C_e and C_o , see section 3. The vertical lines represent the partition of \mathcal{X} in manifolds, see (4.1).

Along the lines of [43, eq. (2.7)], we define $C_e := \{\zeta \in \mathcal{X} \mid \Phi(\zeta, \mathbf{e}) < \Phi(\mathbf{e}, \mathbf{o})\}$ to be the *initial cycle* of \mathbf{e} , that is the maximal cycle that includes \mathbf{e} but does not include \mathbf{o} , namely, it contains all the configurations that can be reached by \mathbf{e} by spending strictly less energy than the one needed for the transition between \mathbf{e} and \mathbf{o} , i.e., the communication height $\Phi(\mathbf{e}, \mathbf{o})$. The corresponding initial cycle of \mathbf{o} is defined analogously and is denoted by C_o .

Given a configuration $\sigma \in \mathcal{X}$, denote by $\Delta H(\sigma)$ the energy difference with respect to either one of the stable states, i.e.,

$$\Delta H(\sigma) := H(\sigma) - H(\mathbf{e}). \tag{3.1}$$

3.1 Odd clusters and regions

For any subset of sites $S \subseteq V$ we define the *complement* of S as $S^c := V \setminus S$, the *external boundary* $\partial^+ S$ as the subset of sites in S^c that are adjacent to a site in S , i.e.,

$$\partial^+ S := \{v \in S^c \mid \exists w \in S : (v, w) \in E\},$$

and ∇S as the subset of edges connecting the sites in S with those in $\partial^+ S$, i.e.,

$$\nabla S := \{(v, w) \in E \mid v \in S, w \in \partial^+ S\}.$$

A (connected) *odd cluster* $C \subseteq V$ is a subset of sites that satisfies both the following conditions:

1. If an odd site $v \in V_e$ belongs to C , then so do the four neighbouring even sites, i.e., $\partial^+ \{v\} \subset C$;
2. $C \cap V_e$ is connected as a sub-graph of the graph (V_e, E^*) , with $E^* := \{(v, w) \in V_e \times V_e \mid d(v, w) = 2\}$, where $d(\cdot, \cdot)$ denotes the usual graph distance on Λ .

We denote by $C_o(\Lambda)$ the collection of odd clusters in Λ .

Consider the dual graph $\Lambda' = (V', E')$ of the graph Λ , which is a discrete torus of the same size. Given an odd cluster C , consider the edge set ∇C that disconnects C from its complement C^c . We associate with ∇C the edge set $\gamma(C) \subset E'$ on the dual graph Λ' which consists of all the edges of Λ' orthogonal to edges in ∇C . Such a set, to which we refer as the *contour* of the cluster C , consists of one or more piecewise linear closed curves and, by construction, $|\gamma(C)| = |\nabla C|$. Leveraging this

fact, we define the *perimeter* $P(C)$ of the odd cluster C as the total length of the contour $\gamma(C)$, i.e.,

$$P(C) := |\gamma(C)|. \tag{3.2}$$

As proved in [57], the perimeter of the odd cluster C satisfies the following identity:

$$P(C) = 4(|C \cap V_e| - |C \cap V_o|). \tag{3.3}$$

We call *area* of an odd cluster C the number of odd occupied sites it comprises. We say that an odd cluster is degenerate if it has area 0 and non-degenerate otherwise.

We introduce a mapping $\mathcal{O} : \mathcal{X} \rightarrow 2^V$ that associates to a given hard-core configuration $\sigma \in \mathcal{X}$ the subset $\mathcal{O}(\sigma) \subseteq V$ defined as

$$\mathcal{O}(\sigma) := \{v \in V_o \mid \sigma(v) = 1\} \cup \{v \in V_e \mid \sigma(v) = 0\}. \tag{3.4}$$

In other words, $\mathcal{O}(\sigma)$ is the subset comprising all occupied odd sites and even empty sites of the configuration σ . It is immediate to check that \mathcal{O} is an injective mapping, and we will refer to the image $\mathcal{O}(\sigma)$ of a configuration σ as its *odd region*.

The odd region $\mathcal{O}(\sigma)$ of a configuration $\sigma \in \mathcal{X}$ can be partitioned into its connected components, say $C_1(\sigma), \dots, C_m(\sigma) \in \mathcal{C}_o(\Lambda)$, for some $m \in \mathbb{N}$, which are, by definition, odd clusters, that is,

$$\mathcal{O}(\sigma) = \bigsqcup_{i=1}^m C_i(\sigma). \tag{3.5}$$

Using the partition (3.5) of the odd region $\mathcal{O}(\sigma)$ into odd clusters, the definitions of contour and perimeter can be extended to the whole odd region in an obvious way, so that we can ultimately define the *contour* $\gamma(\sigma)$ of a configuration $\sigma \in \mathcal{X}$ as

$$\gamma(\sigma) := \bigsqcup_{i=1}^m \gamma(C_i(\sigma)), \tag{3.6}$$

and its *perimeter* $P(\sigma)$ as

$$P(\sigma) := \sum_{i=1}^m P(C_i(\sigma)). \tag{3.7}$$

As shown in [57], starting from (3.3), a double counting argument yields the following identity that relates the perimeter $P(\sigma)$ of a hard-core configuration $\sigma \in \mathcal{X}$ with its energy $H(\sigma)$ (recall (3.1)-(3.2))

$$P(\sigma) = 4 \Delta H(\sigma). \tag{3.8}$$

Given a configuration $\sigma \in \mathcal{X}$, we define the odd non-degenerate region $\mathcal{O}^{nd}(\sigma)$ as a subset of $\mathcal{O}(\sigma)$ containing only odd non-degenerate clusters. See Figure 7 for an example of an odd region and an odd non-degenerate region.

3.2 Odd rhombi

Given an odd site $\eta = (\eta_1, \eta_2) \in V_o$ and two positive integers $\ell_1, \ell_2 \leq L$, the *odd rhombus* $\mathcal{R}_{\ell_1, \ell_2}(\eta)$ with reference site η and lengths ℓ_1 and ℓ_2 is the odd cluster defined as

$$\mathcal{R}_{\ell_1, \ell_2}(\eta) := S_{\ell_1, \ell_2}(\eta) \cup \partial^+ S_{\ell_1, \ell_2}(\eta), \tag{3.9}$$

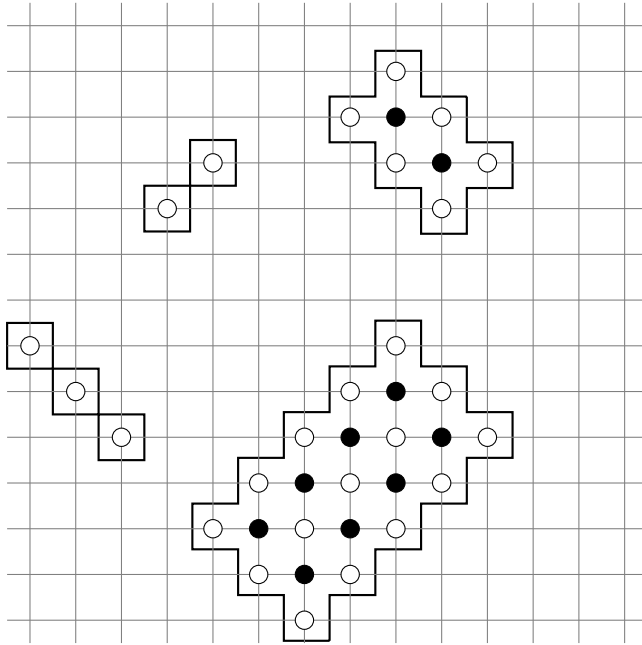


Figure 6. Example of four different rhombi, namely $\mathcal{R}_{1,2}, \mathcal{R}_{4,2}, \mathcal{R}_{0,2}$ and $\mathcal{R}_{1,0}$ (in clockwise order from the top-right corner).

where $S_{\ell_1, \ell_2}(\eta) \subseteq V_{\circ}$ is the subset of odd sites given by

$$\begin{aligned}
 S_{\ell_1, \ell_2}(\eta) &:= \bigcup_{0 \leq k \leq \ell_1 - 1, 0 \leq j \leq \ell_2 - 1} \{(\eta_1 + k + j, \eta_2 + k - j)\} \\
 &= \{v = (v_1, v_2) \in V \mid \exists k \in [[0, \ell_1]], j \in [[0, \ell_2]] : v_1 = \eta_1 + k + j, v_2 = \eta_2 + k - j\}.
 \end{aligned}
 \tag{3.10}$$

In the latter definition, the sums and subtractions of coordinates are taken modulo L . In the case $\ell_1 \ell_2 = 0$, we can take $\eta \in V_{\bullet}$ and define the *degenerate* rhombus $\mathcal{R}_{\ell_1, \ell_2}(\eta)$ as the odd cluster

$$\mathcal{R}_{\ell_1, \ell_2}(\eta) = \begin{cases} \bigcup_{0 \leq j \leq \ell_2} \{(\eta_1 + j, \eta_2 - j)\} & \text{if } \ell_1 = 0 \text{ and } \ell_2 \neq 0, \\ \bigcup_{0 \leq k \leq \ell_1} \{(\eta_1 + k, \eta_2 - k)\} & \text{if } \ell_1 \neq 0 \text{ and } \ell_2 = 0, \\ (\eta_1, \eta_2) & \text{if } \ell_1 = \ell_2 = 0. \end{cases}$$

Note that, in this case, $\mathcal{R}_{\ell_1, \ell_2}(\eta)$ is a subset of even sites. The area of $\mathcal{R}_{\ell_1, \ell_2}(\eta)$ is the cardinality of $S_{\ell_1, \ell_2}(\eta)$ in the non-degenerate case, whereas in the degenerate case it is equal to zero. Some examples of rhombi and degenerate rhombi are shown in Figure 6. We observe that the non-degenerate rhombus $\mathcal{R}_{\ell_1, \ell_2}$ has ℓ_1 diagonals of length ℓ_2 and ℓ_2 diagonals of length ℓ_1 in the opposite direction, which we will refer to as *complete diagonals*. We denote by $\mathbf{R}_{\circ}(\Lambda) \subset \mathbf{C}_{\circ}(\Lambda)$ the collection of all odd rhombi on Λ including the degenerate ones. For every odd cluster $C \in \mathbf{C}_{\circ}(\Lambda)$, we define the *surrounding rhombus* $\mathcal{R}(C)$ as the minimal rhombus (by inclusion) in $\mathbf{R}_{\circ}(\Lambda)$ such that $C \subseteq \mathcal{R}(C)$; see Figure 8 for an example.

Most of the results for odd rhombi that will be proved are translation-invariant, the reason why we will often refer to the rhombus $\mathcal{R}_{\ell_1, \ell_2}(\eta)$ simply as $\mathcal{R}_{\ell_1, \ell_2}$, without explicitly specifying the reference site η . The next two lemmas, Lemmas 3.1 and 3.2, concern the properties of rhombi

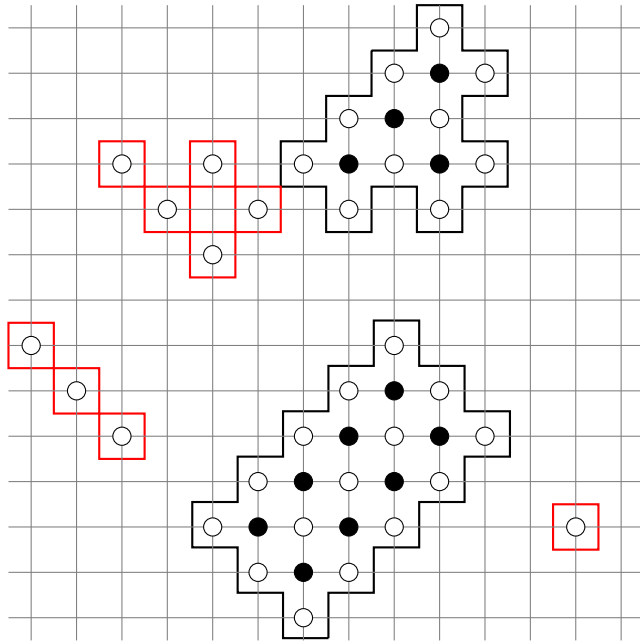


Figure 7. Example of a configuration σ , in which the contour of the non-degenerate (degenerate) odd clusters is highlighted in black (red, respectively). The contour $\gamma(\sigma)$ of the configuration σ is of the odd region $\mathcal{O}(\sigma)$ is the union of black lines (corresponding to $\mathcal{O}^{nd}(\sigma)$) and red lines.

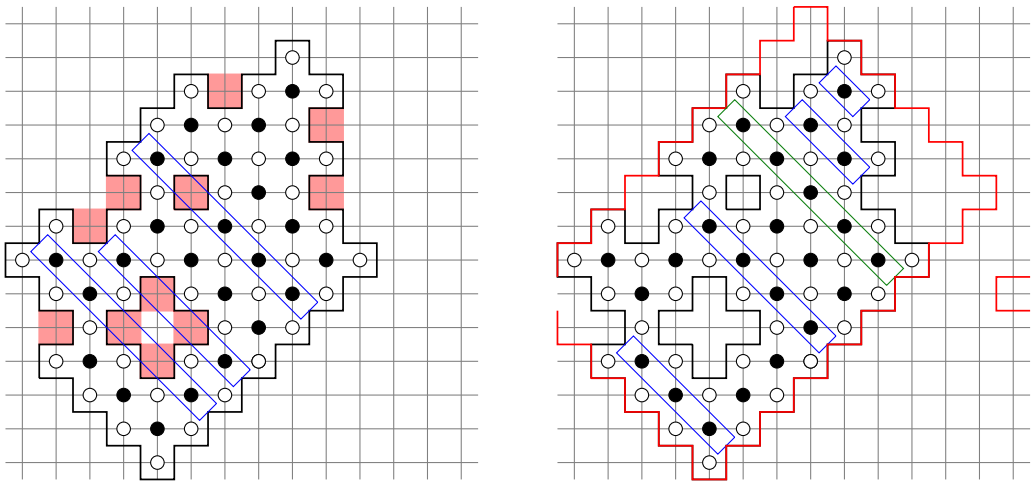


Figure 8. Example of an odd cluster C (on the left) and its surrounding rhombus $\mathcal{R}(C) = \mathcal{R}_{8,5}$ in red (on the right). On the left, the red squares contain the antiknobs and the decreasing broken diagonals are highlighted with blue rectangles. On the right, we highlight the decreasing shorter (resp. complete) diagonals with blue (resp. green) rectangles.

on a square $L \times L$ grid with periodic boundary conditions. Their proofs, being involved but not particularly insightful, are deferred to Appendix A.

Lemma 3.1 (Set of sites winds around the torus). *Given $\eta = (\eta_1, \eta_2) \in V_{\mathbf{o}}$ and two non-negative integers $\ell_1, \ell_2 \leq L$ such that $\ell_1 \leq \ell_2$ and $\ell_1 \geq L/2$, the following statements hold:*

(i) If $\ell_2 \leq L - 2$, then

$$\bigcup_{\substack{0 \leq k \leq \ell_1 \\ \ell_2 + 1 \leq j \leq L - 1}} \{(\eta_1 + k + j - 1, \eta_2 + k - j)\} \cup \bigcup_{\substack{\ell_1 + 1 \leq k \leq L - 1 \\ 0 \leq j \leq \ell_2}} \{(\eta_1 + k + j - 1, \eta_2 + k - j)\} \subseteq \bigcup_{\substack{0 \leq k \leq \ell_1 \\ 0 \leq j \leq \ell_2}} \{(\eta_1 + k + j - 1, \eta_2 + k - j)\}.$$

(ii) If $\ell_2 = L - 1$, then

$$\bigcup_{\substack{\ell_1 + 1 \leq k \leq L - 1 \\ 0 \leq j \leq L - 1}} \{(\eta_1 + k + j - 1, \eta_2 + k - j)\} \subseteq \bigcup_{\substack{0 \leq k \leq \ell_1 \\ 0 \leq j \leq L - 1}} \{(\eta_1 + k + j - 1, \eta_2 + k - j)\} \quad (3.11)$$

and

$$\bigcup_{\substack{L/2 \leq k \leq \ell_1 - 1 \\ 1 \leq j \leq L - 2}} \{(\eta_1 + k + j, \eta_2 + k - j)\} \subseteq \bigcup_{\substack{0 \leq k \leq L/2 - 1 \\ 0 \leq j \leq L - 2}} \{(\eta_1 + k + j, \eta_2 + k - j)\}. \quad (3.12)$$

For any subset of sites $A \subseteq V$, we define the *complement* of A as the complementary set of A in V , i.e., as $V \setminus A$.

Lemma 3.2 (Properties of rhombi). *Given $\eta \in V_{\mathbf{o}}$ and two non-negative integers $\ell_1, \ell_2 \leq L$, the following statements hold:*

- (i) *If $\max\{\ell_1, \ell_2\} \leq L - 2$ and $\min\{\ell_1, \ell_2\} \geq L/2$, then the complement of the rhombus $\mathcal{R}_{\ell_1, \ell_2}(\eta)$ is a rhombus $\mathcal{R}_{L - \ell_1 - 1, L - \ell_2 - 1}(\hat{\eta})$ for some $\hat{\eta} \in V_{\mathbf{e}}$.*
- (ii) *If $\max\{\ell_1, \ell_2\} = L - 1$ and $\min\{\ell_1, \ell_2\} \geq L/2$, then the complement of the rhombus $\mathcal{R}_{\ell_1, \ell_2}(\eta)$ is the disjoint union of $L - \min\{\ell_1, \ell_2\}$ odd sites.*
- (iii) *If $\max\{\ell_1, \ell_2\} = L$ and $\min\{\ell_1, \ell_2\} < L/2$, then the rhombus $\mathcal{R}_{\ell_1, \ell_2}(\eta)$ contains $L \ell_1$ odd sites and $L(\ell_1 + 1)$ even sites.*
- (iv) *If $\max\{\ell_1, \ell_2\} = L$ and $\min\{\ell_1, \ell_2\} \geq L/2$, then the rhombus $\mathcal{R}_{\ell_1, \ell_2}(\eta)$ coincides with V .*

These two lemmas will now be used to prove the next proposition, which gives a formula for the perimeter of a rhombus $\mathcal{R}_{\ell_1, \ell_2}$. To this end, we will use the fact that a rhombus $\mathcal{R}_{\ell_1, \ell_2}$ and its complement in Λ have the same boundary for any $0 \leq \ell_1, \ell_2 \leq L$, and, in particular the same perimeter. In addition, we will say that a rhombus $\mathcal{R}_{\ell_1, \ell_2}$ *winds vertically* (resp. *horizontally*) *around the torus* if there exists a set of $\frac{L}{2}$ odd sites $\eta_1, \dots, \eta_{L/2}$ in $\mathcal{R}_{\ell_1, \ell_2}$ all on the same column (resp. row). If the direction is not relevant, we will simply say that the rhombus *winds around the torus*.

Proposition 3.3 (Formula for rhombus perimeter). *Given a $L \times L$ toric grid graph Λ and any sizes $0 \leq \ell_1, \ell_2 \leq L$, the perimeter of the rhombus $\mathcal{R}_{\ell_1, \ell_2}$ satisfies the following identity*

$$P(\mathcal{R}_{\ell_1, \ell_2}) = 4 \times \begin{cases} \ell_1 + \ell_2 + 1 & \text{if } \min\{\ell_1, \ell_2\} < L/2 \text{ and } \max\{\ell_1, \ell_2\} < L, \\ 2L - (\ell_1 + \ell_2 + 1) & \text{if } \min\{\ell_1, \ell_2\} \geq L/2 \text{ and } \max\{\ell_1, \ell_2\} < L, \\ L & \text{if } \min\{\ell_1, \ell_2\} < L/2 \text{ and } \max\{\ell_1, \ell_2\} = L, \\ 0 & \text{if } \min\{\ell_1, \ell_2\} \geq L/2 \text{ and } \max\{\ell_1, \ell_2\} = L. \end{cases} \quad (3.13)$$

Proof. First of all, we identify which of the conditions in (3.13) imply that a rhombus winds around the torus. Consider the rhombus $\mathcal{R}_{\ell_1, \ell_2}(\eta)$ with $\eta = (\eta_1, \eta_2) \in V_{\mathbf{o}}$. Let $\sigma = (\sigma_1, \sigma_2) \in S_{\ell_1, \ell_2}(\eta)$ be such that $\sigma_2 = \eta_2$ and $d(\eta_1, \sigma_1)$ is the maximal distance along that horizontal axis. Similarly, let $\xi = (\xi_1, \xi_2) \in S_{\ell_1, \ell_2}(\eta)$ be such that $d(\eta_2, \xi_2)$ is the maximal distance along the vertical axis. Recalling (3.10), since $\sigma_2 = \eta_2$, we have $k = j$ for any $k, j = 1, \dots, \ell_{\min} - 1$, where $\ell_{\min} = \min\{\ell_1, \ell_2\}$. Thus, we obtain

$$\sigma_1 = \eta_1 + k + j = \eta_1 + 2(\ell_{\min} - 1), \tag{3.14}$$

where the last equality follows from the fact that the maximal distance along the horizontal axis is precisely the distance between σ_1 and η_1 . We note that if $d(\eta_1, \sigma_1) < L - 2$ then the rhombus does not wind horizontally around the torus. Thus,

$$d(\eta_1, \sigma_1) = 2(\ell_{\min} - 1) < L - 2 \iff \ell_{\min} < \frac{L}{2}. \tag{3.15}$$

Now, consider the distance between η_2 and ξ_2 . Let $\ell_{\max} = \max\{\ell_1, \ell_2\}$. In this case, if $d(\eta_2, \xi_2) \leq L - 2$ then the rhombus does not wind vertically around the torus. Thus, we have

$$d(\eta_2, \xi_2) = \max_{k,j} |\eta_2 - (\eta_2 - k + j)| = \ell_{\max} - 1 \leq L - 2. \tag{3.16}$$

We conclude that if $\ell_{\min} < \frac{L}{2}$ and $\ell_{\max} < L$, then the rhombus does not wind around the torus and the perimeter is the length of its external boundary. In view of (3.3), the claim follows. Otherwise, there are three cases, which will be treated separately:

- (a) $\ell_{\min} \geq \frac{L}{2}$ and $\ell_{\max} \leq L - 2$;
- (b) $\ell_{\min} \geq \frac{L}{2}$ and $\ell_{\max} > L - 2$;
- (c) $\ell_{\min} < \frac{L}{2}$ and $\ell_{\max} = L$.

- (a) Consider the complement of the rhombus $\mathcal{R}_{\ell_1, \ell_2}(\eta)$ for some η . By virtue of Lemma 3.2(i), we know that its complement in V is a rhombus with side lengths $\tilde{\ell}_1 = L - \ell_1 - 1$ and $\tilde{\ell}_2 = L - \ell_1 - 1$. We claim that this complementary rhombus does not wind around the torus. Using condition $\ell_{\min} \geq \frac{L}{2}$, we find that the maximal side length of the complementary rhombus is

$$\max\{\tilde{\ell}_1, \tilde{\ell}_2\} = \max\{L - \ell_1 - 1, L - \ell_2 - 1\} = L - \ell_{\min} - 1 \leq L - \frac{L}{2} - 1 < L, \tag{3.17}$$

that is, $\max\{\tilde{\ell}_1, \tilde{\ell}_2\} < L$. Moreover, the minimal side length is

$$\min\{\tilde{\ell}_1, \tilde{\ell}_2\} = \min\{L - \ell_1 - 1, L - \ell_2 - 1\} = L - \ell_{\max} - 1 \leq L - \ell_{\min} - 1 \leq L - \frac{L}{2} - 1, \tag{3.18}$$

that is, $\min\{\tilde{\ell}_1, \tilde{\ell}_2\} < \frac{L}{2}$. Since the perimeter of the rhombus R_{ℓ_1, ℓ_2} is the same as that of $R_{L-\ell_1-1, L-\ell_2-1}$, the claim follows from (3.3).

- (b) The claim follows from Lemma 3.2(ii)–(iii) and (3.3).
- (c) The claim follows from Lemma 3.2(iv) and (3.3). □

We say that an odd cluster C is *monotone* when its perimeter coincides with that of its surrounding rhombus $\mathcal{R}(C)$ if it does not wind around the torus, i.e., $P(C) = P(\mathcal{R}(C))$. Otherwise, we say that an odd cluster C is monotone when its perimeter coincides with that of a bridge, i.e., $P(C) = 4L$. Note that it immediately follows that a monotone odd cluster C has no *holes*,

i.e., empty odd sites with the four even neighbouring sites belonging to C . An empty odd site $\eta \notin C$ is an *antiknob for the cluster C* if it has at least three neighbouring even empty sites that belong to C . Figure 8 (left) highlights in red the antiknobs of a hard-core configuration.

Given an odd cluster $C \in \mathcal{C}_o(\Lambda)$ and an integer $k \geq 1$, we say that C displays an *increasing* (resp. *decreasing*) *diagonal broken in k sites* if there exist a sequence of sites $z_i = (x_i, y_i) \in V_o \setminus C$, $i = 1, \dots, k$, such that

- $x_{i+1} = x_i + 1$ and $y_{i+1} = y_i + 1$ (resp. $x_{i+1} = x_i + 1$ and $y_{i+1} = y_i - 1$) for any $i = 1, \dots, k - 1$, and
- the two odd sites $(x_1 - 1, y_1 - 1)$ and $(x_k + 1, y_k + 1)$ (resp. $(x_1 - 1, y_1 + 1)$ and $(x_k + 1, y_k - 1)$) belong to the cluster C .

By construction of a broken diagonal, the two sites z_1 and z_k are always antiknobs. If it does not matter if an increasing or decreasing diagonal is broken, we simply say that a diagonal is broken. Broken diagonals are visualized in blue in Figure 8 (left). Given an odd cluster $C \in \mathcal{C}_o(\Lambda)$ and an integer $k \geq 1$, we say that C displays an *increasing* (resp. *decreasing*) *shorter diagonal lacking in k sites* if there exist a sequence of sites $z_i = (x_i, y_i) \in (V_o \cap \mathcal{R}(C)) \setminus C$, $i = 1, \dots, k$, such that

- $x_{i+1} = x_i + 1$ and $y_{i+1} = y_i + 1$ (resp. $x_{i+1} = x_i + 1$ and $y_{i+1} = y_i - 1$) for any $i = 1, \dots, k - 1$, and
- the two odd sites $(x_1 - 1, y_1 - 1)$ and $(x_k + 1, y_k + 1)$ (resp. $(x_1 - 1, y_1 + 1)$ and $(x_k + 1, y_k - 1)$) do not belong to $\mathcal{R}(C)$.

Figure 8 (right) highlights the shorter diagonals in blue.

3.3 Expanding an odd cluster: the filling algorithms

We now describe an iterative procedure that builds a path ω in \mathcal{X} from a configuration σ with a unique odd cluster to another configuration σ' that (i) displays a rhombus, and (ii) whose energy $H(\sigma')$ is equal to or lower than $H(\sigma)$.

The path ω can be described as the concatenation of two paths, each obtained by means of a specific *filling algorithm*. The reason behind this name is that, along the generated paths, any incomplete diagonal in the odd cluster of the starting configuration is gradually filled by adding particles at odd sites until a rhombus is obtained.

The two paths can be intuitively described as follows. The first path, denoted as $\tilde{\omega}$, starts from a configuration with at least one broken diagonal and, by filling one by one all broken diagonals in lexicographic order, arrives at a configuration without broken diagonals. Each broken diagonal is progressively filled by removing a particle in the even site at distance 1 from an antiknob that lies on that diagonal and adding a particle in the odd site where the antiknob is. The antiknobs on the same diagonal are processed in lexicographic order. The second path, denoted as $\bar{\omega}$, starts from a configuration without broken diagonals (such as any ending configuration of the path $\tilde{\omega}$) and arrives at a configuration displaying an odd rhombus. The construction of this second path is similar to that of the first path, but in this case the particles are added in odd sites to fill all the shorter diagonals.

The filling algorithms that generate the two paths $\tilde{\omega}$ and $\bar{\omega}$ are designed so that the maximum energy along the resulting path $\omega = \tilde{\omega} \cup \bar{\omega}$, i.e., Φ_ω , is never larger than $H(\sigma) + 1$. More specifically, the perimeter of the odd cluster either decreases or does not change along $\tilde{\omega}$, whereas it can increase and sequentially decrease by the same amount along $\bar{\omega}$. Proposition 3.4, whose proof is postponed to subsection 5.1, specifies the requirement for the starting configuration and summarizes the properties of the path generated by the filling algorithm.

Algorithm 1: Filling algorithm to build path $\tilde{\omega}$

Input: a configuration $\sigma \in \mathcal{X}$ consisting of a unique odd cluster C with $m \geq 1$ broken diagonals such that the j -th is broken in k_j sites for $j = 1, \dots, m$

Output: $\tilde{\omega} : \sigma \rightarrow \tilde{\sigma}$, with the configuration $\tilde{\sigma} \in \mathcal{X}$ consisting of a unique odd cluster with no broken diagonals

```

 $\sigma_0 = \sigma;$ 
for  $j = 1, \dots, m$  do
     $\sigma_j = \sigma_{j-1};$ 
    for  $i = 1, \dots, k_j$  do
        Consider the  $i$ -th antiknob (in lexicographic order) of the  $j$ -th broken diagonal in  $C$ 
        and denote it by  $x_{j,i} \in V_{\mathbf{o}}$ 
        if  $x_{j,i}$  has a neighboring occupied site  $\tilde{x}_{j,i} \in V_{\mathbf{e}}$  then
             $\tilde{\sigma}_{j,i} = \sigma_j^{(\tilde{x}_{j,i}, 0)};$ 
             $\sigma_{j,i} = \tilde{\sigma}_{j,i}^{(x_{j,i}, 1)};$ 
        else
             $\tilde{\sigma}_{j,i} = \sigma_j^{(x_{j,i}, 1)};$ 
             $\sigma_{j,i} = \tilde{\sigma}_{j,i};$ 
        end
         $\sigma_{j+1} = \sigma_{j,k_j};$ 
         $\tilde{\omega}_{j,i} = (\sigma_j, \tilde{\sigma}_{j,1}, \sigma_{j,1}, \dots, \tilde{\sigma}_{j,i}, \sigma_{j,i});$ 
    end
     $\tilde{\omega}_j = \tilde{\omega}_{j,k_j};$ 
     $\sigma_{j+1} = \sigma_{j,k_j};$ 
end
 $\tilde{\sigma} = \sigma_m;$ 
 $\tilde{\omega}$  is the concatenation of the paths  $\tilde{\omega}_1, \dots, \tilde{\omega}_m$ 

```

To formally define these two algorithms, we introduce the following notation. Given two configurations $\sigma, \sigma' \in \mathcal{X}$ and a subset of sites $W \subset \Lambda$, we write $\sigma|_W = \sigma'|_W$ if $\sigma(v) = \sigma'(v)$ for every $v \in W$. Given a configuration $\sigma \in \mathcal{X}$, we let

- $\sigma^{(v,0)}$ be the configuration $\sigma' \in \mathcal{X}$ such that $\sigma'_{|V \setminus \{v\}} = \sigma_{|V \setminus \{v\}}$ and $\sigma'(v) = 0$; and
- $\sigma^{(v,1)}$ be the configuration $\sigma' \in \mathcal{X}$ such that $\sigma'_{|V \setminus \{v\}} = \sigma_{|V \setminus \{v\}}$ and $\sigma'(v) = 1$.

In general, $\sigma^{(v,1)}$ may not be a hard-core configuration in \mathcal{X} , since σ may already have a particle residing in one of the four neighbouring sites of v .

Algorithm 1 (resp. Algorithm 2) provide the detailed pseudocode for the filling algorithm that yields $\tilde{\omega}$ (resp. $\tilde{\omega}$).

Proposition 3.4 (Odd cluster expansion via filling algorithms). *Let $\sigma, \sigma' \in \mathcal{X}$ be two hard-core configurations on Λ , $\sigma \neq \sigma'$, and \mathcal{R} a rhombus such that*

- (i) *There exists a connected odd cluster $C \subseteq \mathcal{O}(\sigma)$ such that $\mathcal{R}(C) = \mathcal{R}$;*
- (ii) $\sigma|_{\Lambda \setminus \mathcal{R}} = \sigma'|_{\Lambda \setminus \mathcal{R}};$
- (iii) $\sigma'|_{\mathcal{R}} = \mathbf{o}|_{\mathcal{R}}.$

Then, there exists a path $\omega : \sigma \rightarrow \sigma'$ such that $\Phi_\omega - H(\sigma) \leq 1$. In addition, if C has at least one broken diagonal, then $P(\sigma) > P(\sigma')$, otherwise $P(\sigma) = P(\sigma')$.

Algorithm 2: Filling algorithm to build path $\bar{\omega}$

Input: a configuration $\sigma \in \mathcal{X}$ consists of a unique odd cluster C with no broken diagonal and $m \geq 0$ increasing shorter diagonals. The quantity k_j is the difference between the length of the shorter diagonal and the corresponding one of the surrounding rhombus for $j = 1, \dots, m$

Output: $\bar{\omega} : \sigma \rightarrow \bar{\sigma}$, with the configuration $\bar{\sigma} \in \mathcal{X}$ having a unique odd cluster, which is a rhombus

```

if  $m = 0$  then
  |  $\bar{\sigma} = \sigma$  and  $\bar{\omega}$  is trivial;
else
  |  $\sigma_0 = \sigma$ ;
  | for  $j = 1, \dots, m$  do
  |   |  $\sigma_j = \sigma_{j-1}$ ;
  |   | for  $i = 1, \dots, k_j$  do
  |   |   | Consider the  $i$ -th empty odd site (in lexicographic order) not belonging to the  $j$ -th
  |   |   | shorter diagonal in  $C$  but in the corresponding complete diagonal of the
  |   |   | surrounding rhombus and denote it by  $x_{j,i} \in V_o$ 
  |   |   | if  $x_{j,i}$  has a neighboring occupied site  $\bar{x}_{j,i} \in V_e$  then
  |   |   |   |  $\bar{\sigma}_{j,i} = \sigma_j^{(\bar{x}_{j,i},0)}$ ;
  |   |   |   |  $\sigma_{j,i} = \bar{\sigma}_{j,i}^{(x_{j,i},1)}$ ;
  |   |   |   | else
  |   |   |   |   |  $\bar{\sigma}_{j,i} = \sigma_j^{(x_{j,i},1)}$ ;
  |   |   |   |   |  $\sigma_{j,i} = \bar{\sigma}_{j,i}$ ;
  |   |   |   | end
  |   |   |   |  $\sigma_{j+1} = \sigma_{j,k_j}$ ;
  |   |   |   |  $\bar{\omega}_{j,i} = (\sigma_j, \bar{\sigma}_{j,1}, \sigma_{j,1}, \dots, \bar{\sigma}_{j,i}, \sigma_{j,i})$ ;
  |   |   |   | end
  |   |   |   |  $\bar{\omega}_j = \bar{\omega}_{j,k_j}$ ;
  |   |   |   |  $\sigma_{j+1} = \sigma_{j,k_j}$ ;
  |   |   | end
  |   |  $\bar{\sigma} = \sigma_m$ ;
  |   | Obtain  $\bar{\omega}$  as the concatenation of the paths  $\bar{\omega}_1, \dots, \bar{\omega}_m$ 
  | end

```

We note that conditions (i), (ii), and (iii) mean that there is a unique odd cluster in σ different from a rhombus, i.e., there exists at least one broken or shorter diagonal.

Thanks to Proposition 3.4, we are able to characterize the configurations with minimal perimeter for a fixed number of occupied odd sites. This finding is formalized in the following two results, Proposition 3.6 and Corollary 3.7, whose proofs are deferred to subsection 5.1.

To state the precise results, we first introduce the notion of bars as follows. We define a vertical (resp. horizontal) bar B of length k as the union of particles arranged in odd sites x_1, \dots, x_k belonging to the same column (resp. row) such that $d(x_i, x_{i+1}) = 2$ for any $i = 1, \dots, k - 1$. In the case of $k = 1$, we will refer to it as *protuberance*. If in the same column (resp. row) there are m disjoint vertical (resp. horizontal) bars, each of them of length k_i , we say that the total length of the bars is $k = k_1 + \dots + k_m$. Similarly, we can define a *diagonal bar* and note that it can correspond to a shorter or complete diagonal. If it does not matter whether the bar is vertical, horizontal, or diagonal, we simply refer to it as a *bar*. Finally, we will say that a bar B is attached to a cluster C when all the particles belonging to B are at distance two from C . Note that in Figure 8 (right) the

shorter diagonals of lengths three and one are diagonal bars. See Figure 8 (left) for examples of vertical bars.

Lemma 3.5. *For any n positive integer there exist two positive integers s and k , with $0 \leq k < s$, such that either (i) $n = s(s - 1) + k$ or (ii) $n = s^2 + k$.*

Proof. See the first part of [26, Lemma 6.17]. □

Proposition 3.6 (Perimeter-Minimal rhombi). *Consider $n \leq L(L - 2)$ and let s, k be the unique integers as in Lemma 3.5. The set of odd clusters with area n that have minimal perimeter contains either a rhombus $\mathcal{R}_{s,s-1}$ or $\mathcal{R}_{s-1,s}$ with a bar of length k attached to one of its longest sides if $n = s(s - 1) + k$ and a rhombus $\mathcal{R}_{s,s}$ with a bar of length k attached to one of its sides if $n = s^2 + k$.*

Corollary 3.7 (Minimal perimeter). *Consider $n \leq L(L - 2)$ and let s, k be the unique integers as in Lemma 3.5. The perimeter P of an odd cluster with area n satisfies the following inequalities:*

$$\left(\frac{P}{4} - 1\right)^2 \geq \begin{cases} 4n & \text{if } s < L/2, \\ 2(L^2 - 2n) & \text{if } L/2 \leq s < L. \end{cases}$$

In addition, for all $s < L$ we have that

$$P \geq 4(2\sqrt{n} + 1) \tag{3.19}$$

and for $s < \frac{L}{2}$ the equality holds if and only if the odd cluster is the rhombus $\mathcal{R}_{s,s}$.

Lastly, in the next lemma, we derive an isoperimetric inequality assuming the total number of odd and even occupied sites is fixed. To this end, we first define the *real area* of a configuration σ as

$$\tilde{n}(\sigma) = o(\sigma) + \tilde{e}(\sigma), \tag{3.20}$$

where $o(\sigma)$ (resp. $\tilde{e}(\sigma)$) denotes the number of occupied odd (resp. empty even) sites of the configuration σ .

Lemma 3.8 (Perimeter-Minimal rhombi with fixed real area). *Given $1 \leq \ell < \frac{L}{2}$, the unique odd cluster with real area $\tilde{n} = 2\ell^2 + 2\ell + 1$ and minimal perimeter is the rhombus $\mathcal{R}_{\ell,\ell}$. In particular, for $\tilde{n} = \frac{L^2}{2} - L + 1$ this rhombus is $\mathcal{R}_{\frac{L}{2}-1, \frac{L}{2}-1}$.*

We use this lemma to characterize the critical configurations with an odd cluster of rhomboidal shape that does not wind around the torus. Indeed, we identify the shape of protocritical configurations σ with minimal perimeter and fixed real area $\frac{L^2}{2} - L + 1$ such that $\mathcal{R}(\mathcal{O}^{nd}(\sigma))$ does not wind around the torus, and we show that if the trajectory visits another type of configuration with such a real area, then the corresponding path would not be optimal. The proof is given in subsection 5.1.

4. Essential saddles: proof of the main theorem

In this section, we first formally introduce in subsection 4.1 the six sets appearing in the statement of Theorem 2.1 and then prove the same theorem in subsection 4.2 by showing that the elements of those six sets are all essential saddles for the transition from \mathbf{e} to \mathbf{o} .

4.1 Preliminaries

We say that a configuration $\sigma \in \mathcal{X}$ has a *odd (resp. even) vertical bridge* if there exists a column in which the configuration σ perfectly agrees with \mathbf{o} (resp. \mathbf{e}). We define *odd (resp. even) horizontal bridge* in an analogous way and we say that a configuration $\sigma \in \mathcal{X}$ has an *odd (resp. even) cross*

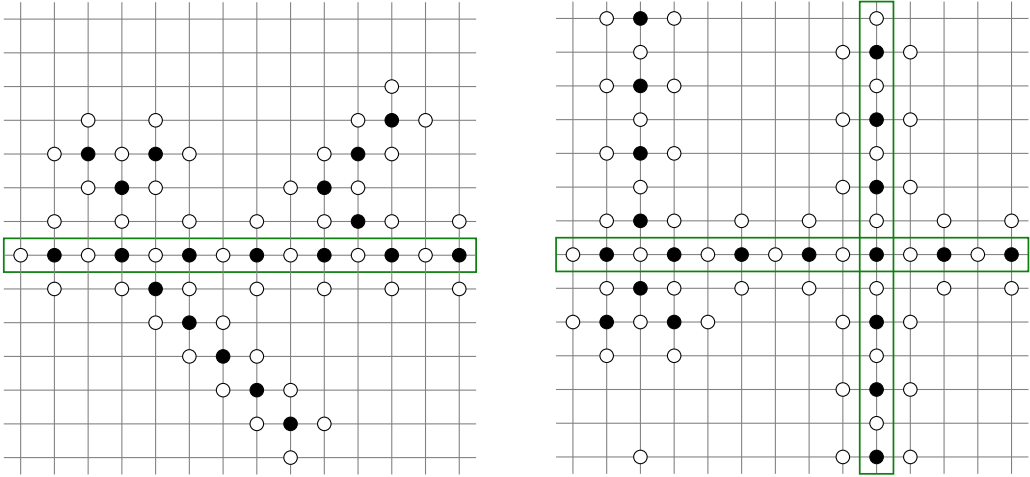


Figure 9. Examples of configurations displaying an odd horizontal bridge (on the left) and an odd cross (on the right).

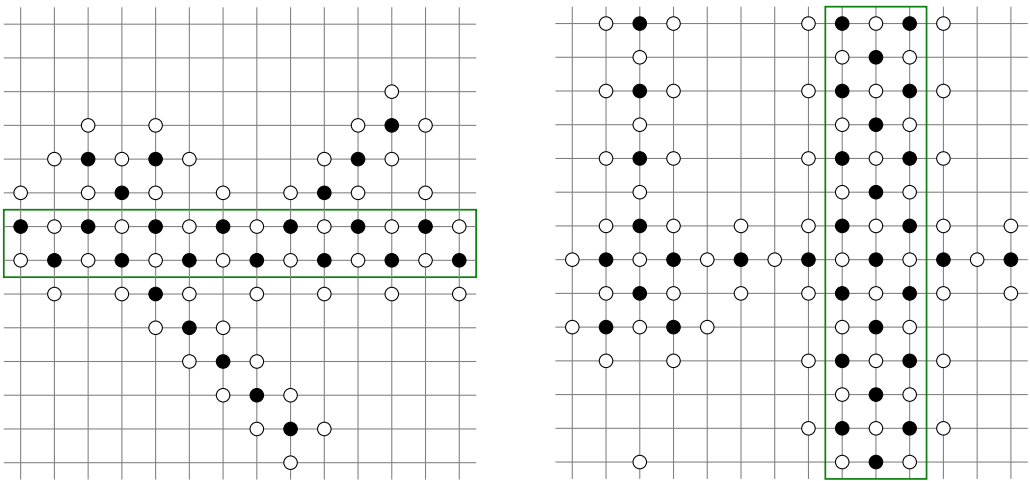


Figure 10. Examples of configurations displaying an odd horizontal double (2-uple) bridge (on the left) and an odd vertical triple (3-uple) bridge (on the right).

if it has both vertical and horizontal odd (resp. even) bridges (see Figure 9). In addition, we say that a configuration displays an *odd (resp. even) vertical m -uple bridge*, with $m \geq 2$, if there exist m contiguous columns in which the configuration perfectly agrees with \mathbf{o} (resp. \mathbf{e}). Similarly, we can define an *odd (resp. even) vertical m -uple bridge* (see Figure 10). We refer to [47] for more details.

The next lemma states that all configurations $\sigma \in \mathcal{X}$ with $\Delta H(\sigma) < L$ must belong to one of the two initial cycles.

Lemma 4.1 (Configurations with $\Delta H < L$ belong to one of the initial cycles). *If a configuration $\sigma \in \mathcal{X}$ is such that $\Delta H(\sigma) < L$, then there exists a path $\omega : \sigma \rightarrow \{\mathbf{e}, \mathbf{o}\}$ with $\Phi_\omega \leq H(\sigma) + 1$. In particular, either $\sigma \in C_e$ or $\sigma \in C_o$.*

Proof. If $\Delta H(\sigma) < L$, then there exists both a horizontal and a vertical bridge. Due to the hard-core constraints, these $L - 1$ particles should all reside at sites of the same parity. Hence, σ has

either an even cross or an odd cross. Then, using the *reduction algorithm* introduced in [47], one can build a path to either \mathbf{e} or \mathbf{o} , respectively, with the desired properties. \square

Definition 4.2. A hard-core configuration $\sigma \in \mathcal{X}$ on the $L \times L$ toric grid graph Λ belongs to $C_{ir}(\mathbf{e}, \mathbf{o})$ if the following conditions hold:

1. the odd region $\mathcal{O}(\sigma)$ contains only a non-degenerate cluster C and a degenerate rhombus $D \in \{\mathcal{R}_{1,0}, \mathcal{R}_{0,1}\}$ at distance two from C ;
2. the cluster C is monotone;
3. C is a rhombus $\mathcal{R}_{\frac{L}{2}-1, \frac{L}{2}-1}$;
4. $\sigma_{|\Lambda \setminus (C \cup D)} = \mathbf{e}_{|\Lambda \setminus (C \cup D)}$.

See Figure 2 (left) for an example of configurations in $C_{ir}(\mathbf{e}, \mathbf{o})$.

Definition 4.3. A hard-core configuration $\sigma \in \mathcal{X}$ on the $L \times L$ toric grid graph Λ belongs to $C_{gr}(\mathbf{e}, \mathbf{o})$ (resp. $C_{cr}(\mathbf{e}, \mathbf{o})$) if the following conditions hold:

1. the odd region $\mathcal{O}(\sigma)$ contains only a non-degenerate cluster C and a degenerate rhombus $D = \mathcal{R}_{0,0}$ at distance one from an antiknob;
2. the cluster C is monotone;
3. C is a rhombus $\mathcal{R}_{\frac{L}{2}-1, \frac{L}{2}-1}$ (resp. $\mathcal{R}_{\frac{L}{2}-1, \frac{L}{2}}$) with a single bar of length k , for $k = 1, \dots, \frac{L}{2} - 1$ (resp. $k = 1, \dots, \frac{L}{2} - 2$), attached to one of its sides;
4. $\sigma_{|\Lambda \setminus (C \cup D)} = \mathbf{e}_{|\Lambda \setminus (C \cup D)}$.

See Figure 2 (right) and Figure 3 (left) for an example of configurations in $C_{gr}(\mathbf{e}, \mathbf{o})$ and $C_{cr}(\mathbf{e}, \mathbf{o})$, respectively. Note that for any $\sigma \in C_{ir}(\mathbf{e}, \mathbf{o}) \cup C_{gr}(\mathbf{e}, \mathbf{o})$ the surrounding rhombus $R(\mathcal{O}(\sigma))$ is $\mathcal{R}_{\frac{L}{2}-1, \frac{L}{2}}$, while for any $\sigma \in C_{cr}(\mathbf{e}, \mathbf{o})$ the surrounding rhombus $R(\mathcal{O}(\sigma))$ is $\mathcal{R}_{\frac{L}{2}, \frac{L}{2}}$.

Definition 4.4. A hard-core configuration $\sigma \in \mathcal{X}$ on the $L \times L$ toric grid graph Λ belongs to $C_{sb}(\mathbf{e}, \mathbf{o})$ if the following conditions hold:

1. the odd region $\mathcal{O}(\sigma)$ contains only a non-degenerate cluster C and a degenerate region D consisting of two even sites at distance one from the same antiknob;
2. the cluster C is monotone;
3. C is a single column or row of length $\frac{L}{2} - 1$;
4. $\sigma_{|\Lambda \setminus (C \cup D)} = \mathbf{e}_{|\Lambda \setminus (C \cup D)}$.

Note that the unique possibilities are that (i) D consists of two degenerate rhombi $\mathcal{R}_{0,0}$ as in Figure 3 (right) or (ii) $D \in \{\mathcal{R}_{0,1}, \mathcal{R}_{1,0}\}$ as in Figure 11 (left).

Definition 4.5. A hard-core configuration $\sigma \in \mathcal{X}$ on the $L \times L$ toric grid graph Λ belongs to $C_{mb}(\mathbf{e}, \mathbf{o})$ if the following conditions hold:

1. the odd region $\mathcal{O}(\sigma)$ contains only a non-degenerate cluster C and a degenerate rhombus $D = \mathcal{R}_{0,0}$ at distance one from an antiknob;
2. the cluster C is monotone;
3. C is composed either by:

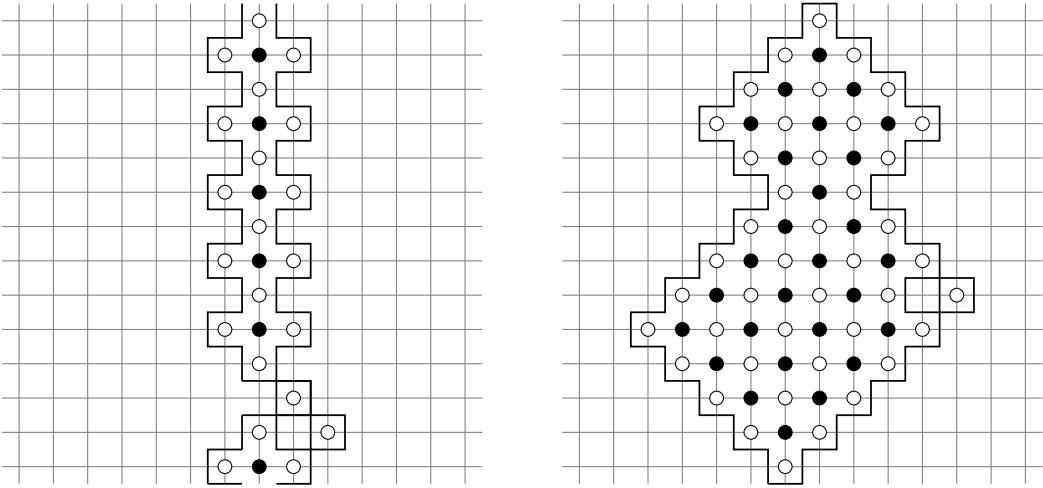


Figure 11. An example of a configuration in $\mathcal{C}_{sb}(\mathbf{e}, \mathbf{o})$ that communicates with $\mathcal{C}_{ib}(\mathbf{e}, \mathbf{o})$ and not with $\mathcal{C}_{mb}(\mathbf{e}, \mathbf{o})$ (on the left) and an example of a configuration in $\mathcal{C}_{ib}(\mathbf{e}, \mathbf{o})$ (on the right).

- a odd $(L - 3)$ -uple bridge, or
- an odd m -uple bridge, with $2 \leq m < L - 3$, together with disjoint bars attached to either side of the m -uple bridge with total length k , with $k = 0, \dots, \frac{L}{2} - 1$, or
- an odd bridge, together with disjoint bars attached to the bridge with total length k , for $k = 0, \dots, \frac{L}{2} - 1$, and C does not contain $\mathcal{R}_{\frac{L}{2}-1, \frac{L}{2}}$;

4. $\sigma_{|\Lambda \setminus (C \cup D)} = \mathbf{e}_{|\Lambda \setminus (C \cup D)}$.

See Figure 4 (left) for an example of a configuration in $\mathcal{C}_{mb}(\mathbf{e}, \mathbf{o})$. Note that any configuration $\sigma \in \mathcal{C}_{mb}(\mathbf{e}, \mathbf{o})$ is such that $\mathcal{R}(\mathcal{O}(\sigma))$ winds around the torus. Thus, the assumption that the non-degenerate cluster C is monotone implies that in condition 3 not every choice of the bars is allowed. Indeed, in order for the cluster to be monotone, the bars on the right (resp. left) of the m -uple bridge can be adjacent only to a longer (resp. shorter) bar in lexicographic order. This implies that all bridges are in contiguous rows or columns. Furthermore, the length of a bar is inversely proportional to its distance from the nearest bar composing the bridge.

Definition 4.6. A hard-core configuration $\sigma \in \mathcal{X}$ on the $L \times L$ toric grid graph Λ belongs to $\mathcal{C}_{ib}(\mathbf{e}, \mathbf{o})$ if the following conditions hold:

1. the odd region $\mathcal{O}(\sigma)$ contains only a non-degenerate cluster C and a degenerate rhombus $D = \mathcal{R}_{0,0}$ at distance one from an antiknob;
2. the cluster C is monotone and does not contain $\mathcal{R}_{\frac{L}{2}-1, \frac{L}{2}-1}$;
3. C is composed either by:
 - one column (or row) B with $\frac{L}{2} - 1$ particles in odd sites or
 - two neighbouring columns (or row) B with $\frac{L}{2} - 1$ particles in odd sites each;
 In addition, in the other columns (or rows) there are k particles arranged in odd sites, for $k = 0, \dots, \frac{L}{2} - 1 - j$, where j is the distance from B ;
4. $\mathcal{R}(C)$ is not contained in $\mathcal{R}_{\frac{L}{2}-1, \frac{L}{2}-1}$;
5. $\sigma_{|\Lambda \setminus (C \cup D)} = \mathbf{e}_{|\Lambda \setminus (C \cup D)}$.

See Figure 4 (right) and Figure 11 (right) for examples of configurations in $\mathcal{C}_{ib}(\mathbf{e}, \mathbf{o})$.

Next, we provide several results investigating the main properties of the optimal paths connecting \mathbf{e} to \mathbf{o} . To this end, we introduce the following partition in *manifolds* of the state space \mathcal{X} : for every $m = -\frac{L^2}{2}, \dots, \frac{L^2}{2}$ we define the *manifold* as the subset of configurations where the difference $m(\sigma) := -e(\sigma) + o(\sigma)$ between odd and even occupied sites is equal to $m \in \mathbb{N}$, i.e.,

$$\mathcal{V}_m := \{\sigma \in \mathcal{X} \mid m(\sigma) = m\}, \tag{4.1}$$

where $e(\sigma) := \sum_{v \in V_e} \sigma(v)$ (resp. $o(\sigma) := \sum_{v \in V_o} \sigma(v)$) is the number of the even (resp. odd) occupied sites in σ .

Lemma 4.7. *For any hard-core configuration $\sigma \in \mathcal{X}$, the following properties hold:*

- (a) *The only configurations accessible from σ with a single nontrivial step of the dynamics belong to $\mathcal{V}_{m(\sigma)-1} \cup \mathcal{V}_{m(\sigma)+1}$. In particular, any path from \mathbf{e} to \mathbf{o} must intersect each manifold \mathcal{V}_m at least once for every $m = -\frac{L^2}{2}, \dots, \frac{L^2}{2}$.*
- (b) *The quantities $m(\sigma)$ and $\Delta H(\sigma)$ always have the same parity, i.e., $m(\sigma) \equiv \Delta H(\sigma) \pmod{2}$.*

The proof of (a) is immediate by noticing that at every step of the dynamics either $e(\sigma)$ or $o(\sigma)$ can change value and at most by ± 1 and that of (b) follows from the fact that $\Delta H(\sigma) = -e(\sigma) - o(\sigma) + \frac{L^2}{2}$ and that L is even.

A special role in our analysis will be played by the *non-backtracking paths*, i.e., those paths that visit each manifold exactly once. Lemmas 4.8–4.10 below ensure the existence of a optimal path connecting \mathbf{e} to \mathbf{o} , which can be constructed as a suitable composition of the paths described below, and passing through the six sets that define $\mathcal{C}^*(\mathbf{e}, \mathbf{o})$. The optimality of this path is guaranteed by the conditions on the height of each path described below. In addition, Lemma 4.11 below shows that some of the sets composing $\mathcal{C}^*(\mathbf{e}, \mathbf{o})$ do not communicate directly. Later, in subsection 4.2.2, combining these lemmas, we will show that the communication structure of these six sets at energy not higher than $H(\mathbf{e}) + L + 1$ is the one illustrated in Figure 5. The proof of these lemmas is deferred to subsection 5.2.

Lemma 4.8. *The following statements hold.*

- (i) *For any configuration $\eta \in \mathcal{C}_{ir}(\mathbf{e}, \mathbf{o})$ there exists a non-backtracking path $\omega : \mathbf{e} \rightarrow \eta$ such that $\Phi_\omega - H(\mathbf{e}) = \Delta H(\eta) = L + 1$ and $\arg \max_{\xi \in \omega} \Delta H(\xi) = \{\eta\}$.*
- (ii) *For any configuration $\eta \in \mathcal{C}_{sb}(\mathbf{e}, \mathbf{o})$ there exists a non-backtracking path $\omega : \mathbf{e} \rightarrow \eta$ such that $\Phi_\omega - H(\mathbf{e}) = \Delta H(\eta) = L + 1$ and $\arg \max_{\xi \in \omega} \Delta H(\xi) = \{\eta\}$.*

Lemma 4.9. *The following statements hold.*

- (i) *For any configuration $\eta \in \mathcal{C}_{ib}(\mathbf{e}, \mathbf{o})$ there exist a configuration $\bar{\eta} \in \mathcal{C}_{sb}(\mathbf{e}, \mathbf{o})$ and a non-backtracking path $\omega : \bar{\eta} \rightarrow \eta$ such that $\Phi_\omega - H(\mathbf{e}) = \Delta H(\eta) = L + 1$ and $\arg \max_{\xi \in \omega} H(\xi) \subseteq \mathcal{C}_{sb}(\mathbf{e}, \mathbf{o}) \cup \mathcal{C}_{ib}(\mathbf{e}, \mathbf{o})$.*
- (ii) *For any configuration $\eta \in \mathcal{C}_{gr}(\mathbf{e}, \mathbf{o})$ there exist a configuration $\bar{\eta} \in \mathcal{C}_{ir}(\mathbf{e}, \mathbf{o})$, a configuration $\tilde{\eta} \in \mathcal{C}_{ib}(\mathbf{e}, \mathbf{o})$ and two non-backtracking paths $\omega : \bar{\eta} \rightarrow \eta$, $\omega' : \tilde{\eta} \rightarrow \eta$ such that*
 - $\Phi_\omega - H(\mathbf{e}) = L + 1$ and $\arg \max_{\xi \in \omega} H(\xi) \subseteq \mathcal{C}_{gr}(\mathbf{e}, \mathbf{o}) \cup \mathcal{C}_{ir}(\mathbf{e}, \mathbf{o})$;
 - $\Phi_{\omega'} - H(\mathbf{e}) = L + 1$ and $\arg \max_{\xi \in \omega'} H(\xi) \subseteq \mathcal{C}_{gr}(\mathbf{e}, \mathbf{o}) \cup \mathcal{C}_{ib}(\mathbf{e}, \mathbf{o})$.
- (iii) *For any configuration $\eta \in \mathcal{C}_{mb}(\mathbf{e}, \mathbf{o})$ there exist a configuration $\bar{\eta} \in \mathcal{C}_{sb}(\mathbf{e}, \mathbf{o})$, a configuration $\tilde{\eta} \in \mathcal{C}_{ib}(\mathbf{e}, \mathbf{o})$ and two non-backtracking paths $\omega : \bar{\eta} \rightarrow \eta$, $\omega' : \tilde{\eta} \rightarrow \eta$ such that*

- $\Phi_\omega - H(\mathbf{e}) = L + 1$ and $\arg \max_{\xi \in \omega} H(\xi) \subseteq C_{mb}(\mathbf{e}, \mathbf{o}) \cup C_{sb}(\mathbf{e}, \mathbf{o})$;
 - $\Phi_{\omega'} - H(\mathbf{e}) = L + 1$ and $\arg \max_{\xi \in \omega'} H(\xi) \subseteq C_{mb}(\mathbf{e}, \mathbf{o}) \cup C_{ib}(\mathbf{e}, \mathbf{o})$.
- (iv) For any configuration $\eta \in C_{cr}(\mathbf{e}, \mathbf{o})$ there exist a configuration $\bar{\eta} \in C_{gr}(\mathbf{e}, \mathbf{o})$, a configuration $\tilde{\eta} \in C_{mb}(\mathbf{e}, \mathbf{o})$ and two non-backtracking paths $\omega : \bar{\eta} \rightarrow \eta$, $\omega' : \tilde{\eta} \rightarrow \eta$ such that
- $\Phi_\omega - H(\mathbf{e}) = L + 1$ and $\arg \max_{\xi \in \omega} H(\xi) \subseteq C_{cr}(\mathbf{e}, \mathbf{o}) \cup C_{gr}(\mathbf{e}, \mathbf{o})$;
 - $\Phi_{\omega'} - H(\mathbf{e}) = L + 1$ and $\arg \max_{\xi \in \omega'} H(\xi) \subseteq C_{cr}(\mathbf{e}, \mathbf{o}) \cup C_{mb}(\mathbf{e}, \mathbf{o})$.

Lemma 4.10. *The following statements hold.*

- (i) For any configuration $\eta \in C_{cr}(\mathbf{e}, \mathbf{o})$ there exists a non-backtracking path $\omega : \eta \rightarrow \mathbf{o}$ such that $\Phi_\omega - H(\mathbf{e}) = L + 1$ and $\arg \max_{\xi \in \omega} H(\xi) \subseteq C_{cr}(\mathbf{e}, \mathbf{o})$.
- (ii) For any configuration $\eta \in C_{mb}(\mathbf{e}, \mathbf{o})$ there exists a non-backtracking path $\omega : \eta \rightarrow \mathbf{o}$ such that $\Phi_\omega - H(\mathbf{e}) = L + 1$ and $\arg \max_{\xi \in \omega} H(\xi) \subseteq C_{mb}(\mathbf{e}, \mathbf{o})$.

Lemma 4.11. *The following statements hold.*

- (i) For any configurations $\eta \in C_{ir}(\mathbf{e}, \mathbf{o})$ and $\eta' \in C_{ib}(\mathbf{e}, \mathbf{o})$, there is no optimal path $\omega : \eta \rightarrow \eta'$ such that $\arg \max_{\xi \in \omega} \subseteq C_{ir}(\mathbf{e}, \mathbf{o}) \cup C_{ib}(\mathbf{e}, \mathbf{o})$.
- (ii) For any configurations $\eta \in C_{ib}(\mathbf{e}, \mathbf{o})$ and $\eta' \in C_{cr}(\mathbf{e}, \mathbf{o})$, there is no optimal path $\omega : \eta \rightarrow \eta'$ such that $\arg \max_{\xi \in \omega} \subseteq C_{cr}(\mathbf{e}, \mathbf{o}) \cup C_{ib}(\mathbf{e}, \mathbf{o})$.
- (iii) For any configurations $\eta \in C_{ir}(\mathbf{e}, \mathbf{o})$ and $\eta' \in C_{mb}(\mathbf{e}, \mathbf{o})$, there is no optimal path $\omega : \eta \rightarrow \eta'$ such that $\arg \max_{\xi \in \omega} \subseteq C_{ir}(\mathbf{e}, \mathbf{o}) \cup C_{mb}(\mathbf{e}, \mathbf{o})$.
- (iv) For any configurations $\eta \in C_{gr}(\mathbf{e}, \mathbf{o})$ and $\eta' \in C_{mb}(\mathbf{e}, \mathbf{o})$, there is no optimal path $\omega : \eta \rightarrow \eta'$ such that $\arg \max_{\xi \in \omega} \subseteq C_{gr}(\mathbf{e}, \mathbf{o}) \cup C_{mb}(\mathbf{e}, \mathbf{o})$.

4.2 Proof of Theorem 2.1

This section is entirely devoted to the proof of Theorem 2.1. More specifically, we prove that any essential saddle belongs to the set $C^*(\mathbf{e}, \mathbf{o})$ in subsection 4.2.1, we describe how the transitions between essential gates can take place in subsection 4.2.2, and we prove that all the saddles in $C^*(\mathbf{e}, \mathbf{o})$ are essential in subsection 4.2.3.

4.2.1 Every essential saddle belongs to $C^*(\mathbf{e}, \mathbf{o})$

In this subsection, we will show that any essential saddle σ belongs to the subset $C^*(\mathbf{e}, \mathbf{o})$. This readily follows from Proposition 4.12 below.

Proposition 4.12. *Let σ be an essential saddle. Then, the following statements hold:*

- (i) If $\mathcal{R}(\mathcal{O}^{nd}(\sigma))$ and $\mathcal{R}(\mathcal{O}(\sigma))$ do not wind around the torus, then $\sigma \in C_{ir}(\mathbf{e}, \mathbf{o}) \cup C_{gr}(\mathbf{e}, \mathbf{o})$.
- (ii) If $\mathcal{R}(\mathcal{O}^{nd}(\sigma))$ does not wind around the torus, $\mathcal{R}(\mathcal{O}(\sigma))$ does, and σ belongs to $\omega \in (\mathbf{e} \rightarrow \mathbf{o})_{opt}$ that crosses the set $C_{ir}(\mathbf{e}, \mathbf{o}) \cup C_{gr}(\mathbf{e}, \mathbf{o})$, then $\sigma \in C_{cr}(\mathbf{e}, \mathbf{o})$.
- (iii) If $\mathcal{R}(\mathcal{O}^{nd}(\sigma))$ does not wind around the torus, $\mathcal{R}(\mathcal{O}(\sigma))$ does, and σ belongs to $\omega \in (\mathbf{e} \rightarrow \mathbf{o})_{opt}$ that does not cross the set $C_{ir}(\mathbf{e}, \mathbf{o}) \cup C_{gr}(\mathbf{e}, \mathbf{o})$, then $\sigma \in C_{sb}(\mathbf{e}, \mathbf{o}) \cup C_{ib}(\mathbf{e}, \mathbf{o})$.
- (iv) If $\mathcal{R}(\mathcal{O}^{nd}(\sigma))$ winds around the torus, then $\sigma \in C_{mb}(\mathbf{e}, \mathbf{o})$.

We observe that these four cases (i)–(iv) listed in Proposition 4.12 cover all possibilities and thus form a partition of the set $\mathcal{G}(\mathbf{e}, \mathbf{o})$ of essential saddles for the transitions $\mathbf{e} \rightarrow \mathbf{o}$.

Before presenting the proof, note that given a configuration $\sigma \in \mathcal{S}(\mathbf{e}, \mathbf{o})$, if we know on which manifold \mathcal{V}_m it lies, then the quantities $e(\sigma)$ and $o(\sigma)$ are uniquely determined and can be explicitly calculated as

$$o(\sigma) = \frac{m}{2} + \frac{L^2}{4} - \frac{L+1}{2} \quad \text{and} \quad e(\sigma) = -\frac{m}{2} + \frac{L^2}{4} - \frac{L+1}{2}. \tag{4.2}$$

This readily follows from the fact that $\Delta H(\sigma) = L + 1 = -e(\sigma) - o(\sigma) + \frac{L^2}{2}$ and $m = -e(\sigma) + o(\sigma)$. Furthermore, since $\sigma \in \mathcal{S}(\mathbf{e}, \mathbf{o})$, $\Delta H(\sigma) = L + 1$ and m have to be odd integers by Lemma 4.7(b).

To prove Proposition 4.12, we make use of an additional lemma (whose proof is deferred to subsection 5.3), which characterizes the intersection between any optimal path and a specific manifold, namely \mathcal{V}_{m^*} with $m^* := 3 - L$.

Lemma 4.13 (Geometrical properties of the saddles on the manifold \mathcal{V}_{m^*}). *Any non-backtracking optimal path $\omega : \mathbf{e} \rightarrow \mathbf{o}$ visits a configuration $\sigma \in \mathcal{V}_{m^*}$ that satisfy one of the following properties:*

- (i) *If both $\mathcal{R}(\mathcal{O}^{nd}(\sigma))$ and $\mathcal{R}(\mathcal{O}(\sigma))$ do not wind around the torus, then $\sigma \in \mathcal{C}_{ir}(\mathbf{e}, \mathbf{o})$.*
- (ii) *If $\mathcal{R}(\mathcal{O}^{nd}(\sigma))$ does not wind around the torus but $\mathcal{R}(\mathcal{O}(\sigma))$ does, then $\sigma \in \mathcal{C}_{ib}(\mathbf{e}, \mathbf{o})$.*
- (iii) *If both $\mathcal{R}(\mathcal{O}^{nd}(\sigma))$ and $\mathcal{R}(\mathcal{O}(\sigma))$ wind around the torus, then $\sigma \in \mathcal{C}_{mb}(\mathbf{e}, \mathbf{o})$.*

Proof of Proposition 4.12.

Case (i). Let σ be an essential saddle such that $\mathcal{R}(\mathcal{O}^{nd}(\sigma))$ and $\mathcal{R}(\mathcal{O}(\sigma))$ do not wind around the torus. If $\sigma \in \mathcal{V}_{m^*}$, by Lemma 4.13(i) we know that $\sigma \in \mathcal{C}_{ir}(\mathbf{e}, \mathbf{o})$. Otherwise, we assume that $\sigma \notin \mathcal{V}_{m^*}$. First, we observe that $\sigma \notin \mathcal{V}_m$ with $m < m^*$, otherwise the saddle σ is not essential. Indeed, every optimal path from \mathbf{e} to \mathbf{o} has to cross a configuration $\bar{\sigma} \in \mathcal{V}_{m^*}$ in $\mathcal{C}_{ir}(\mathbf{e}, \mathbf{o})$ due to Lemma 4.13(i). Thus, we can write a general optimal path $\omega = (\mathbf{e}, \omega_1, \dots, \omega_k, \sigma, \dots, \bar{\sigma}, \omega_{k+1}, \dots, \omega_{k+m}, \mathbf{o})$ and define the path $\omega' = (\mathbf{e}, \tilde{\omega}_1, \dots, \tilde{\omega}_n, \bar{\sigma}, \omega_{k+1}, \dots, \omega_{k+m}, \mathbf{o})$, where $\arg \max_{\xi \in \{\mathbf{e}, \tilde{\omega}_1, \dots, \tilde{\omega}_n, \bar{\sigma}\}} H(\xi) = \{\bar{\sigma}\}$. This path ω' exists thanks to Lemma 4.8(i). Thus, we are left to analyse the case $\sigma \in \mathcal{V}_m$ with $m > m^*$. We need to show that any essential saddle crossed afterward belongs to the set $\mathcal{C}_{gr}(\mathbf{e}, \mathbf{o})$. Using again Lemma 4.13, the path ω crosses a configuration $\sigma \in \mathcal{C}_{ir}(\mathbf{e}, \mathbf{o})$ to reach \mathbf{o} . Starting from it, there is a unique possible move to lower the energy towards \mathbf{o} along the path ω , that is adding a particle in the unique unblocked empty odd site. Afterward, the unique possible move is to remove a particle from an even site. If this site is at a distance greater than one from an antiknob, then there is no more allowed move. Otherwise, the resulting configuration belongs to the set $\mathcal{C}_{gr}(\mathbf{e}, \mathbf{o})$. By iterating this pair of moves until the shorter diagonal of the rhombus is completely filled, we find that all the saddles that are crossed belong to $\mathcal{C}_{gr}(\mathbf{e}, \mathbf{o})$. Moreover, from this point onward, it is only possible to remove a particle from an even site at distance one from the antiknob, obtaining a configuration in $\mathcal{C}_{gr}(\mathbf{e}, \mathbf{o}) \cap \mathcal{V}_1$.

Case (ii). By assumption, the path ω crosses the set $\mathcal{C}_{ir}(\mathbf{e}, \mathbf{o}) \cup \mathcal{C}_{gr}(\mathbf{e}, \mathbf{o})$. Without loss of generality, we may consider ω as a non-backtracking path. If this is not the case, we can apply the following argument to the last configuration visited by the path in the manifold \mathcal{V}_{m^*} . In particular, in view of the properties of the path ω shown in case (i), we know that the last configuration crossed in $\mathcal{C}_{gr}(\mathbf{e}, \mathbf{o})$ belongs to \mathcal{V}_1 and it is composed of a unique non-degenerate cluster $\mathcal{R}_{\frac{L}{2}-1, \frac{L}{2}}$ with a degenerate cluster $\mathcal{R}_{0,0}$ at distance one from the antiknob. Starting from it, there is a unique possible move to lower the energy towards \mathbf{o} along the path ω , that is, adding a particle in the unique unblocked empty odd site. Afterward, the unique possible move is to remove a particle from an even site. The resulting configuration is in $\mathcal{C}_{cr}(\mathbf{e}, \mathbf{o})$. By iterating this pair of moves until

the shorter diagonal of the rhombus is completely filled, we find that all the saddles that are crossed belong to $\mathcal{C}_{cr}(\mathbf{e}, \mathbf{o})$.

Case (iii). As in case (ii), we assume that the path ω is non-backtracking. By assumption, the path ω does not cross the set $\mathcal{C}_{ir}(\mathbf{e}, \mathbf{o}) \cup \mathcal{C}_{gr}(\mathbf{e}, \mathbf{o})$, thus for Lemma 4.13(ii) the path crosses the set $\mathcal{C}_{ib}(\mathbf{e}, \mathbf{o})$, say in configuration $\bar{\eta}$. Let $\mathcal{V}_{\bar{m}}$ the first manifold containing a configuration in $\mathcal{C}_{ib}(\mathbf{e}, \mathbf{o})$.

Consider first the case in which the saddle σ is crossed by the path ω on the manifolds \mathcal{V}_m , with $\bar{m} \leq m < m^*$. Since ω crosses the set $\mathcal{C}_{ib}(\mathbf{e}, \mathbf{o})$, we will show that the saddle σ belongs to the set $\mathcal{C}_{sb}(\mathbf{e}, \mathbf{o}) \cup \mathcal{C}_{ib}(\mathbf{e}, \mathbf{o})$. To this end, we need to consider the time-reversal of the path $\omega = (\mathbf{e}, \omega_1, \dots, \omega_k, \bar{\eta}, \dots, \mathbf{o})$, where $\bar{\eta} \in \mathcal{C}_{ib}(\mathbf{e}, \mathbf{o})$. Starting from $\bar{\eta}$, since $\Delta H(\bar{\eta}) = L + 1$, the energy of configuration ω_k is less than that of $\bar{\eta}$. Moreover, the unique possible move is to add a particle in the unique empty even site at distance one from an antiknob. Then, the unique possible move from ω_k to ω_{k-1} is to remove a particle from an occupied odd site. The configuration ω_{k-1} belongs to the set $\mathcal{C}_{sb}(\mathbf{e}, \mathbf{o})$ if it contains at least one bridge, otherwise, it belongs to the set $\mathcal{C}_{ib}(\mathbf{e}, \mathbf{o})$. By iterating this argument, we obtain the desired claim.

Consider now the case in which the saddle σ is crossed by the path ω on the manifolds \mathcal{V}_m , with $m > m^*$. Since ω crosses the set $\mathcal{C}_{ib}(\mathbf{e}, \mathbf{o})$, we will show that the saddle σ belongs to the set $\mathcal{C}_{sb}(\mathbf{e}, \mathbf{o}) \cup \mathcal{C}_{ib}(\mathbf{e}, \mathbf{o})$. Note that the unique admissible moves are the following: add a particle in the antiknob and then remove a particle from an even site at distance one from an antiknob. By iterating this couple of moves, we get that the resulting configuration belongs to the set $\mathcal{C}_{ib}(\mathbf{e}, \mathbf{o})$ since $\mathcal{R}(\mathcal{O}^{nd}(\sigma))$ does not wind around the torus.

It remains to consider the case $\sigma \in \mathcal{V}_m$, with $m < \bar{m}$. We will prove that any such σ is not essential. Indeed, any non-backtracking optimal path that visits a configuration in $\mathcal{C}_{ib}(\mathbf{e}, \mathbf{o})$ has crossed a configuration in $\mathcal{C}_{sb}(\mathbf{e}, \mathbf{o})$ before, by using the same argument as in case (iii) of this proof for $\bar{m} \leq m < m^*$. Thus, we can write $\omega = (\mathbf{e}, \omega_1, \dots, \omega_k, \sigma, \dots, \tilde{\sigma}, \dots, \bar{\sigma}, \omega_{k+1}, \dots, \omega_{k+m}, \mathbf{o})$ and define the path $\omega' = (\mathbf{e}, \omega'_1, \dots, \omega'_n, \tilde{\sigma}, \dots, \bar{\sigma}, \omega_{k+1}, \dots, \omega_{k+m}, \mathbf{o})$, where $\tilde{\sigma}$ is a configuration in $\mathcal{C}_{sb}(\mathbf{e}, \mathbf{o})$, $\bar{\sigma} \in \mathcal{V}_{\bar{m}}$ is a configuration in $\mathcal{C}_{ib}(\mathbf{e}, \mathbf{o})$ thanks to Lemma 4.13(ii) and $\arg \max_{\xi \in \{\mathbf{e}, \omega'_1, \dots, \omega'_n, \tilde{\sigma}\}} H(\xi) = \{\tilde{\sigma}\}$. This path ω' exists thanks to Lemma 4.8(ii) and this concludes case (iii).

Case (iv). By Lemma 4.13(iii), we know that any optimal path $\omega \in (\mathbf{e} \rightarrow \mathbf{o})_{\text{opt}}$ crosses the manifold \mathcal{V}_{m^*} in a configuration $\bar{\sigma}$ belonging to the set $\mathcal{C}_{mb}(\mathbf{e}, \mathbf{o})$.

If the essential saddle $\sigma \in \mathcal{V}_{m^*}$, then we deduce that $\sigma \in \mathcal{C}_{mb}(\mathbf{e}, \mathbf{o})$.

Suppose now that the saddle σ belongs to the manifold \mathcal{V}_m , with $m > m^*$. Starting from such a saddle $\bar{\sigma}$, there is a unique possible move to lower the energy towards \mathbf{o} along the path ω , that is, add a particle to the unique unblocked empty odd site. Afterward, the unique possible move is to remove a particle from an even site. If this site is at a distance greater than one from an antiknob, then there is no more possible move to reach \mathbf{o} in such a way that the path ω is optimal. Otherwise, the resulting configuration belongs to the set $\mathcal{C}_{mb}(\mathbf{e}, \mathbf{o})$. Indeed, by construction, we deduce that the resulting non-degenerate odd cluster is still monotone due to the properties of the bars attached to each bridge. By iterating this pair of moves until there is a row or a column that is not a bridge, we obtain that all the saddles that are crossed belong to $\mathcal{C}_{mb}(\mathbf{e}, \mathbf{o})$. Finally, from this point onward, it is only possible to remove a particle from an even site at distance one from the antiknob, obtaining the last configuration in $\mathcal{C}_{mb}(\mathbf{e}, \mathbf{o})$. Afterward, the energy only decreases and therefore no more saddles are crossed.

Suppose now that the saddle σ belongs to the manifold \mathcal{V}_m , with $m < m^*$. Note that, starting from such $\bar{\sigma} \in \mathcal{C}_{mb}(\mathbf{e}, \mathbf{o})$, the unique admissible moves to get σ are the following: add a particle to the unique empty even site at distance one from an antiknob and afterward remove a particle from an occupied odd site. By iterating this couple of moves, we get that the resulting configuration belongs to the set $\mathcal{C}_{mb}(\mathbf{e}, \mathbf{o})$ as long as $\mathcal{R}(\mathcal{O}^{nd}(\sigma))$ winds around the torus, otherwise the saddle σ does not satisfy the properties in the statement. \square

4.2.2 Communications between essential gates

In this subsection, we show that the six subsets composing the set $C^*(\mathbf{e}, \mathbf{o})$ communicate as illustrated in Figure 5. The next proposition makes it precise.

Proposition 4.14. *Any non-backtracking optimal path $\omega : \mathbf{e} \rightarrow \mathbf{o}$ crosses the set $C^*(\mathbf{e}, \mathbf{o})$ in one of the following ways:*

- (i) ω passes first through $C_{ir}(\mathbf{e}, \mathbf{o})$, then through $C_{gr}(\mathbf{e}, \mathbf{o})$, and finally through $C_{cr}(\mathbf{e}, \mathbf{o})$;
- (ii) ω passes first through $C_{sb}(\mathbf{e}, \mathbf{o})$, then through $C_{ib}(\mathbf{e}, \mathbf{o})$ and afterwards through $C_{gr}(\mathbf{e}, \mathbf{o}) \cup C_{mb}(\mathbf{e}, \mathbf{o})$. If ω passes $C_{gr}(\mathbf{e}, \mathbf{o})$, then it eventually has to visit $C_{cr}(\mathbf{e}, \mathbf{o})$, otherwise it does not have to;
- (iii) ω passes first through $C_{sb}(\mathbf{e}, \mathbf{o})$ and then through $C_{mb}(\mathbf{e}, \mathbf{o})$.

Proof. Consider a non-backtracking optimal path $\omega : \mathbf{e} \rightarrow \mathbf{o}$. If ω visits at least one essential saddle, then we conclude using Proposition 4.12. Thus, suppose that ω visits unessential saddles only, say $\sigma_1, \dots, \sigma_n$. By definition of unessential saddle, we know that there exists another optimal path $\omega' : \mathbf{e} \rightarrow \mathbf{o}$ such that $S(\omega') \subseteq \{\sigma_1, \dots, \sigma_{n-1}\}$, say $S(\omega') \subseteq \{\sigma_1, \dots, \sigma_m\}$ with $m \leq n - 1$. Iterating this argument, we deduce that there exists an optimal path $\bar{\omega} : \mathbf{e} \rightarrow \mathbf{o}$ such that $S(\bar{\omega}) = \{\sigma_1\}$ and this is a contradiction with the assumption that σ_1 is an unessential saddle. Thus, we conclude that any optimal path $\omega : \mathbf{e} \rightarrow \mathbf{o}$ visits the set $C^*(\mathbf{e}, \mathbf{o})$. It remains to prove that the entrance in $C^*(\mathbf{e}, \mathbf{o})$ occurs in one of the ways described in (i)–(iii), which easily follows by combining Lemmas 4.8–4.11. □

4.2.3 All the saddles in $C^*(\mathbf{e}, \mathbf{o})$ are essential

In this first part of the proof, we will prove that every $\sigma \in C^*(\mathbf{e}, \mathbf{o})$ is an essential saddle by constructing a non-backtracking optimal path $\omega : \mathbf{e} \rightarrow \mathbf{o}$ that visits σ .

Leveraging the fact that $\sigma \in C^*(\mathbf{e}, \mathbf{o})$, we construct the desired non-backtracking path ω as a concatenation of two paths as follows. First, using a suitable concatenation of the paths described in Lemmas 4.9–4.10, we can define a path ω_1 that starts from the considered configuration σ to the initial cycle C_e . We then construct another path ω_2 that goes from σ to the target cycle C_o as a suitable concatenation of the paths described in Lemmas 4.8–4.9. The desired non-backtracking path ω is the time-reversal of ω_1 concatenated with ω_2 and it is easy to show that it is also optimal.

Assume now by contradiction that σ is not essential, which means that there must exist another optimal path $\omega' \in (\mathbf{e} \rightarrow \mathbf{o})_{opt}$ such that $S(\omega') \subset S(\omega) \setminus \{\sigma\}$. Recall that by Lemma 4.7(a), such a path ω' that avoids σ still needs to visit the manifold $\mathcal{V}_{m(\sigma)}$ where σ lives at least once. Let η be any such configuration in $\mathcal{V}_{m(\sigma)} \cap \omega'$. We claim that such a configuration η must satisfy

$$\Delta H(\eta) \equiv 1 \pmod{2}.$$

This claim readily follows from Lemma 4.7(b) in combination with the facts that L is even and $\Delta H(\sigma) = L + 1$ by construction.

If $\Delta H(\eta) \geq L + 3$, then ω' is not an optimal path, since $\Phi_{\omega'} - H(\mathbf{e}) \geq L + 3 > L + 1 = \Phi(\mathbf{e}, \mathbf{o}) - H(\mathbf{e})$.

On the other hand, if $\Delta H(\eta) \leq L - 1$, then from Lemma 4.1 it follows that η belongs to one of the two initial cycles. Proposition 4.14 ensures that every non-backtracking optimal path crosses $C^*(\mathbf{e}, \mathbf{o})$ in one of the three ways (i)–(iii) described therein, so that also the optimal path ω' passing through η has to visit $C^*(\mathbf{e}, \mathbf{o})$. Since, by assumption, the path ω' has to avoid the saddle σ , we deduce that there exists another saddle $\tilde{\eta}$ obtained starting from η that does not belong to $\mathcal{V}_{m(\sigma)}$. In particular, the two paths cross the set $C^*(\mathbf{e}, \mathbf{o})$ in three different ways according to Proposition 4.14(i)–(iii). Thus, we deduce that $S(\omega') \not\subset S(\omega) \setminus \{\sigma\}$.

Thus, in view of the parity of $\Delta H(\eta)$, we must have $\Delta H(\eta) = L + 1$, but then η is a saddle and, by construction, it did not belong to $S(\omega)$ and thus $S(\omega') \not\subset S(\omega) \setminus \{\sigma\}$.

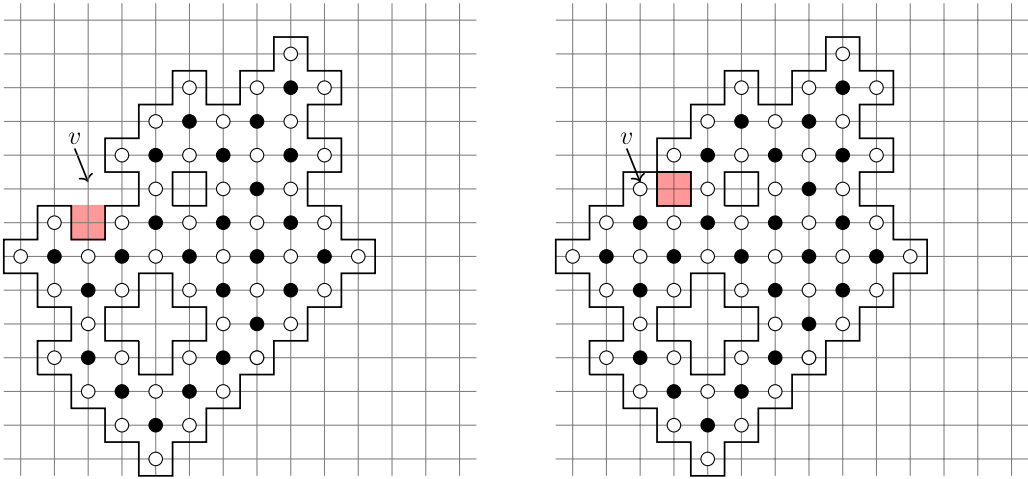


Figure 12. Example of a configuration σ as in the statement of Proposition 3.4 (on the left), where we highlight in red the site containing the target antiknob, and the configuration obtained from σ by filling it after removing a particle from the even site v (on the right), with highlighted in red the site containing the next target antiknob.

5. Proof of auxiliary results

In this section, we give the proof of some auxiliary results stated in Sections 3–4.

5.1 Results on the perimeter of an odd region

Proof of Proposition 3.4. The proof revolves around the simple idea that using the filling algorithms introduced in subsection 3.3 we can expand the odd cluster C (i.e., progressively increase the number of the occupied odd sites in C) in such a way that \mathcal{R} remains the surrounding rhombus and the energy of all configurations along such a path never exceeds $H(\sigma) + 1$. Since by assumption $\sigma \neq \sigma'$, the odd cluster C cannot coincide with \mathcal{R} , in view of conditions (i), (ii), and (iii). Thus, C contains at least a broken diagonal or a shorter diagonal than those of the surrounding rhombus.

We can define the desired path ω as the concatenation of the two paths returned by the filling algorithms $\tilde{\omega}$ and $\bar{\omega}$. If C has no broken diagonal, we take $\tilde{\omega}$ empty. If C has no shorter diagonal, then C already has the shape of a rhombus, and therefore we take $\bar{\omega}$ empty. By the definition of these two paths, the energy increases by one only if an even site has to be emptied, but all these moves are followed by the addition of a particle in an antiknob. Therefore, the energy along the path ω increases by at most one with respect to the starting configuration σ . This procedure ends when C coincides with \mathcal{R} , which implies that the resulting configuration is σ' .

To conclude the proof, we need to show the properties claimed for the perimeter of σ . If C contains $m \geq 1$ broken diagonals, we argue as follows. Since the cluster C is connected, all the empty odd sites in which the diagonals are broken are antiknobs, i.e., they have $n \in \{3, 4\}$ neighbouring even sites belonging to C , see Figure 12. We distinguish the following two cases. If $n = 3$, then we first need to remove a particle from the unique neighbouring occupied even site, like the site v represented in Figure 12 on the left.

After that move, when the particle is added in the antiknob, the perimeter does not change in view of (3.3), otherwise if $n = 4$ then the perimeter decreases (see Figure 12 on the right). This also occurs when we add a particle in the target antiknobs except the last antiknob to obtain the complete diagonal, for which by construction, we have that the perimeter decreases by 4. By iterating this argument for every broken diagonal, we get

$$P(\sigma) \geq P(\tilde{\sigma}) + 4m > P(\tilde{\sigma}).$$

If C does not contain any broken diagonal, we argue as follows. By construction, we deduce that the first odd site we will fill, which is the nearest neighbour of the first shorter diagonal, has three neighbouring even sites belonging to C . Thus, we need to remove a particle from the unique occupied neighbouring even site and then, when the first particle is added to the unique possible antiknob, the perimeter does not change thanks to (3.3). This also occurs when we iterate this argument. \square

Proof of Proposition 3.6. Given any n positive number, let C be an odd cluster with area n . If the cluster C is not connected, by (3.3) it directly follows that C cannot minimize the perimeter of an odd cluster with n particles. Indeed, when the cluster is not connected, the cardinality of $C \cap V_e$ decreases, while the cardinality of $C \cap V_o$ is fixed equal to n . Consider now a connected cluster C . First, we will show that the minimal perimeter is that of the surrounding rhombus. To this end, we consider separately the following three cases:

1. There exists at least one broken diagonal. In this case, we have that $P(C) > P(\mathcal{R}(C))$ by applying Proposition 3.4.
2. There is no broken diagonal, but there exists at least one shorter diagonal with respect to those of the surrounding rhombus. In this case, we have that $P(C) = P(\mathcal{R}(C))$ by applying Proposition 3.4.
3. All diagonals have the same length as those of the surrounding rhombus, namely, all the diagonals are complete. In this case $C = \mathcal{R}(C)$, so it is trivial that $P(C) = P(\mathcal{R}(C))$.

Lastly, we need to show that the minimizing rhombus is either $\mathcal{R}_{s-1,s}$ or $\mathcal{R}_{s,s-1}$ if $n = s(s-1) + k$ and $\mathcal{R}_{s,s}$ if $n = s^2 + k$. We argue by induction over n . If $n = 1$, then it is trivial that the rhombus $\mathcal{R}_{1,1}$ minimizes the perimeter and $n = 1$ can be represented in the form $s(s-1) + k$ choosing $s = 1$ and $k = 0$. Suppose now $n > 1$ and that the claim is true for any $m < n$. Suppose that $n - 1$ can be written as $s(s-1) + k$. In the other case, where $n = s^2 + k$, we can argue in a similar way. If $n - 1 = s(s-1) + k$, with $0 \leq k \leq s - 2$ (resp. $k = s - 1$), then either the rhombus $\mathcal{R}_{s,s-1}$ or $\mathcal{R}_{s-1,s}$ (resp. the rhombus $\mathcal{R}_{s,s}$) minimizes the perimeter of an odd cluster with n particles. Indeed, in any other case, the surrounding rhombus could be either $\mathcal{R}_{s+1,s-1}$ or $\mathcal{R}_{s-1,s+1}$, which has a strictly greater perimeter in view of (3.13). Note that assumption $n \leq L(L-2)$ is needed to avoid rhombi with a maximal side equal to L , because in view of (3.13) we would lose the uniqueness of the minimizing configuration. \square

Proof of Corollary 3.7. We first consider the case in which the area n is of the form $n = s(s-1) + k$. If $s < L/2$, we have that the perimeter of the odd cluster is $P = 4(2s + 1)$. Since the cluster is contained in a rhombus $\mathcal{R}_{s,s}$, we have that $n \leq s^2$ and, hence, $(\frac{P}{4} - 1)^2 \geq 4n$. If $L/2 \leq s < L$, then the perimeter of the odd cluster is $P = 4(2L - 2s - 1)$. Since the cluster is contained in a rhombus $\mathcal{R}_{s,s}$ and therefore the complement in V is a rhombus $\mathcal{R}_{L-s-1,L-s-1}$, we have that $n \geq \frac{L^2}{2} - (L - s - 1)^2$. Hence

$$\left(\frac{P}{4} - 1\right)^2 = 4(L - s - 1)^2 \geq 2(L^2 - 2n).$$

Consider now the other case, when the area n is of the form $n = s^2 + k$. If $s < L/2$ we have that the perimeter of the odd cluster is $P = 4(2s + 2)$. Since the cluster is contained in a rhombus either $\mathcal{R}_{s+1,s}$ or $\mathcal{R}_{s,s+1}$, we have that $n \leq s^2 + s$. Thus, it holds

$$\left(\frac{P}{4} - 1\right)^2 = (2s + 1)^2 = 4(s^2 + s) + 1 \geq 4n + 1.$$

If $L/2 \leq s < L$, then the perimeter of the odd cluster is $P = 4(2L - 2s - 2)$. Since the cluster is contained in either a rhombus $\mathcal{R}_{s+1,s}$ or $\mathcal{R}_{s,s+1}$ and therefore the complement in V is either a rhombus $\mathcal{R}_{L-s-2,L-s-1}$ or $\mathcal{R}_{L-s-1,L-s-2}$, we have that $n \geq \frac{L^2}{2} - (L - s - 1)(L - s - 2)$. Hence,

$$\left(\frac{P}{4} - 1\right)^2 = (2L - 2s - 3)^2 = 4(L - s - 1)(L - s - 2) + 1 \geq 4\left(\frac{L^2}{2} - n\right) + 1 = 2(L^2 - 2n) + 1.$$

Using condition $n \leq L(L - 2)$, inequality (3.19) directly follows. □

Proof of Lemma 3.8. Let σ be a configuration with real area $\tilde{n} = 2\ell^2 + 2\ell + 1$. First, we suppose that the set of odd clusters in σ is composed only of $j \geq 2$ non-degenerate clusters. Each of them has area n_i and perimeter p_i for $i = 1, \dots, j$. Suppose by contradiction that σ has minimal perimeter so that the area of the configuration σ is $n_\sigma = \sum_{i=1}^j n_i$ and its perimeter is $p_\sigma = 4(2\sqrt{n_\sigma} + 1)$. By (3.19), we have $p_i \geq 4(2\sqrt{n_i} + 1)$ for any $i = 1, \dots, j$. Then we obtain that

$$p_\sigma = \sum_{i=1}^j p_i \geq \sum_{i=1}^j 4(2\sqrt{n_i} + 1) \geq 8\sqrt{\sum_{i=1}^j n_i} + 4j \geq 8\left(\sqrt{\sum_{i=1}^j n_i + 1}\right) = 4(2\sqrt{n_\sigma} + 2), \tag{5.1}$$

that is a contradiction.

Second, we suppose that the set of odd clusters in σ is composed of $k \geq 1$ degenerate clusters and of $j \geq 1$ non-degenerate clusters. Each of these non-degenerate clusters has area n_i and perimeter p_i for $i = 1, \dots, j$, so that $n_\sigma = \sum_{i=1}^j n_i$. We denote by \tilde{p}_i for $i = 1, \dots, k$ the perimeter of a degenerate cluster. Suppose by contradiction that σ has minimal perimeter. By (3.19), we have $p_i \geq 4(2\sqrt{n_i} + 1)$ for any $i = 1, \dots, j$ and $p_\sigma = 4(2\sqrt{n_\sigma} + 1)$. Thus, we obtain

$$p_\sigma = \sum_{i=1}^j p_i + \sum_{i=1}^k \tilde{p}_i \geq \sum_{i=1}^j 4(2\sqrt{n_i} + 1) + 4k \geq 8\sqrt{\sum_{i=1}^j n_i} + 4j + 4k \geq 8\sqrt{\sum_{i=1}^j n_i + 4} + 4 = 4(2\sqrt{n_\sigma} + 2), \tag{5.2}$$

that is a contradiction. Thus, we obtain that $k = 0$ and $j = 1$. Since the real area \tilde{n} of the configuration σ is fixed, then also the area n_σ is fixed. Thus, given that σ contains only one non-degenerate cluster with minimal perimeter and with fixed area, by Corollary 3.7 we obtain that the non-degenerate cluster is the rhombus $\mathcal{R}_{\ell,\ell}$, which has precisely real area \tilde{n} . □

5.2 Results on optimal reference paths

Proof of Lemma 4.8. We start by proving (i). The desired path $\omega = (\mathbf{e}, \omega_1, \dots, \omega_{k(L)}, \eta)$ is obtained as follows. Starting from \mathbf{e} , define the configuration ω_1 as that in which one particle is removed from an empty even site, say $v_1 \in V_e$. Similarly, we define ω_2 as the configuration in which a particle is removed from a site $v_2 \in V_e$ such that $d(v_1, v_2) = 2$. Similarly, by removing the particles in $v_3, v_4 \in V_e$ in such a way $d(v_i, v_j) = 2$ for any $i, j = 1, \dots, 4$ and $i \neq j$, we define the configurations ω_3 and ω_4 . Note that $\Delta H(\omega_4) = 4 < L + 1$. Thus, we can define the configuration ω_5 as that obtained from ω_4 by adding a particle to the unique unblocked odd site, i.e., the one at distance one from v_i for any $i = 1, \dots, 4$. See Figure 13 on the left.

We obtain that $\Delta H(\omega_5) = 3 < L + 1$ and ω_5 is composed of a unique non-degenerate odd cluster, which is $\mathcal{R}_{1,1}$. To define the configuration ω_6 , we remove a particle from a site $v_5 \in V_e$ such that $d(v_i, v_5) = 2$ for two indices $i = 1, \dots, 4$. Similarly, we define ω_7 in such a way there is an empty odd site with all the neighbouring even sites that are empty, see Figure 13 in the middle.

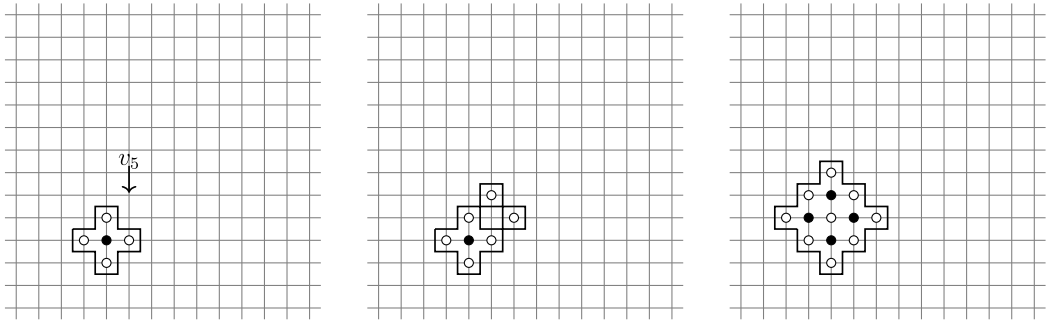


Figure 13. Example of the configurations ω_5 (on the left), ω_7 (in the middle) and ω_{13} (on the right) visited by the path described in the proof of Lemma 4.8(i).

Note that $\Delta H(\omega_7) = 5 < L + 1$. Then, we define ω_8 by adding a particle in the unique unblocked odd site, so that $\Delta H(\omega_8) = 4 < L + 1$. Note that ω_8 contains an odd cluster $\mathcal{R}_{1,2}$. By growing the odd cluster in a spiral fashion, emptying the even sites that are strictly necessary, note that the configuration ω_{13} contains only the non-degenerate cluster $\mathcal{R}_{2,2}$ (see Figure 13 on the right). Then, our path visits all the configurations which have a unique non-degenerate odd cluster C such that $C = \mathcal{R}_{\ell,\ell}$ and $C = \mathcal{R}_{\ell,\ell+1}$ for any $3 \leq \ell \leq \frac{L}{2} - 1$ up to the configuration $\omega_{k(L)-1}$, whose unique non-degenerate odd cluster is $C = \mathcal{R}_{\frac{L}{2}-1, \frac{L}{2}-1}$. Then, the configuration $\omega_{k(L)}$ is defined by removing a particle from an even site w at distance two from C . Finally, the configuration η is obtained by removing a particle from an even site at distance two from C and from w . Since the procedure we defined is invariant by translation, given a fixed configuration $\eta \in \mathcal{C}_{ir}(\mathbf{e}, \mathbf{o})$ is possible to choose the position of the odd clusters in such a way the final configuration of the path we described coincides with the desired η . It remains to show that $\arg \max_{\xi \in \omega} H(\xi) = \{\eta\}$. To this end, since $\Delta H(\eta) = L + 1$ and therefore $\Delta H(\omega_{k(L)}) = L$ and $\Delta H(\omega_{k(L)-1}) = L - 1$, we need only to show that

$$\max_{\xi \in \{\mathbf{e}, \omega_1, \dots, \omega_{k(L)-2}\}} H(\xi) < L + 1.$$

First, we will show that $\Delta H(\eta) = 3 + 2(\ell - 1)$ by induction over the dimension $\ell = 1, \dots, \frac{L}{2} - 1$ of the rhombus $\mathcal{R}_{\ell,\ell}$ composing the unique odd cluster of the configurations η visited by ω . We have already proven the desired property in the case $\ell = 1$. Suppose now that the claim holds for ℓ , with $1 \leq \ell \leq \frac{L}{2} - 2$, thus we will prove that it holds also for $\ell + 1$. To reach the configuration displaying the rhombus $\mathcal{R}_{\ell,\ell+1}$ starting from $\mathcal{R}_{\ell,\ell}$, we need first to remove particles from two even sites by increasing the energy by two. Then, we sequentially add a particle in an odd site and remove a particle in an even site until the length of the shorter diagonal is $\ell - 1$. Finally, the last move is the addition of a particle in an odd site without the need to remove any particle from an even site. Starting from $\mathcal{R}_{\ell,\ell+1}$, to obtain $\mathcal{R}_{\ell+1,\ell+1}$ we follow the same sequence of moves. Thus, for a configuration η containing as unique odd cluster a rhombus $\mathcal{R}_{\ell+1,\ell+1}$ we deduce that $\Delta H(\eta) = 3 + 2(\ell - 1) + 2$, which proves our claim for $\ell + 1$. Along the sequence of moves from $\mathcal{R}_{\ell,\ell}$ to $\mathcal{R}_{\ell+1,\ell+1}$, the energy is at most $3 + 2(\ell - 1) + 3$, which is strictly less than $L + 1$ for $\ell \leq \frac{L}{2} - 1$. Note that we do not to consider the case $\ell = \frac{L}{2} - 2$, indeed the path ω stops before reaching the rhombus $\mathcal{R}_{\frac{L}{2}-1, \frac{L}{2}}$. This concludes the proof of (i).

Now, we prove (ii). The desired path $\omega = (\mathbf{e}, \omega_1, \dots, \omega_{k(L)}, \eta)$ is obtained as follows. Starting from \mathbf{e} , define the configuration ω_1 as that in which one particle is removed from an empty even site, say $v_1 \in V_{\mathbf{e}}$. Similarly, we define ω_2 as the configuration in which a particle is removed from a site $v_2 \in V_{\mathbf{e}}$ such that $d(v_1, v_2) = 2$. Similarly, by removing particles in $v_3, v_4 \in V_{\mathbf{e}}$ in such a way $d(v_i, v_j) = 2$ for any $i, j = 1, \dots, 4$ and $i \neq j$, we define the configurations ω_3 and ω_4 . Note that

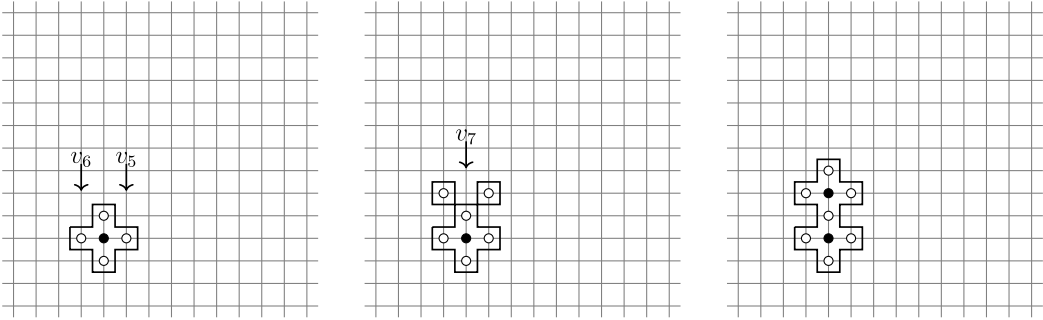


Figure 14. Example of the configurations ω_5 (on the left), ω_7 (in the middle) and ω_9 (on the right) visited by the path described in the proof of Lemma 4.8(ii).

$\Delta H(\omega_4) = 4 < L + 1$. Thus, we can define the configuration ω_5 as the one obtained from ω_4 by adding a particle in the unique unblocked odd site, i.e., the one at distance one from v_i for any $i = 1, \dots, 4$. We obtain that $\Delta H(\omega_5) = 3 < L + 1$ and ω_5 is composed of a unique non-degenerate odd cluster, which is $\mathcal{R}_{1,1}$, see Figure 14 on the left.

Next, we describe four steps that are used in the following iteration. The first step is to define the configuration ω_6 by removing a particle from a site $v_5 \in V_e$ such that $d(v_i, v_5) = 2$ for two indices $i = 1, \dots, 4$. The second step is to remove a particle from a site $v_6 \in V_e$ in such a way there is an empty odd site with two neighbouring empty even sites and the other one is occupied. In this way, we obtain the configuration ω_7 (see Figure 14 in the middle). The third step is to obtain the configuration ω_8 by removing the particle in the site $v_7 \in V_e$ such that $d(v_7, v_5) = d(v_7, v_6) = 2$. Note that $\Delta H(\omega_8) = 6 < L + 1$. Then, the last step is to define ω_9 by adding a particle in the unique unblocked odd site, so that $\Delta H(\omega_9) = 5 < L + 1$ and the energy cost of these four steps is 2. Note that ω_9 is composed of a non-degenerate odd cluster with two odd particles along either the same column or the same row, see Figure 14 on the right.

From this point on, we iterate these four steps for other $\frac{L}{2} - 3$ times, until we obtain the configuration $\omega_{k(L)-1}$ in which either a column or a row contains $\frac{L}{2} - 1$ odd particles. Note that $\Delta H(\omega_{k(L)-1}) = 5 + 2(\frac{L}{2} - 3) = L - 1$. Then, we repeat the first two steps described above and reach the configuration $\eta \in \mathcal{C}_{sb}(\mathbf{e}, \mathbf{o})$ with $\Delta H(\eta) = L + 1$. It is easy to check that $\arg \max_{\xi \in \omega} = \{\eta\}$. Indeed, we get

$$\begin{aligned} \Delta H(\omega_i) &= \Delta H(\omega_{i-1}) + 1 && \text{if } 1 \leq i \leq 4, \\ \Delta H(\omega_{2i-1}) &= \Delta H(\omega_{2i}) - 1 && \text{if } 3 \leq i \leq \frac{k(L)}{2}, \\ \Delta H(\omega_{2i}) &= \Delta H(\omega_{2i-1}) + 3 && \text{if } 3 \leq i \leq \frac{k(L)}{2} - 1, \\ \Delta H(\omega_{k(L)}) &= \Delta H(\omega_{k(L)-1}) + 2, \end{aligned}$$

which concludes the proof of (ii). □

Proof of Lemma 4.9. We start by proving (i). Take the path described in Lemma 4.8(ii) until it visits for the first time a configuration in $\mathcal{C}_{sb}(\mathbf{e}, \mathbf{o})$ as in Figure 11 on the left. Starting from such a configuration, add a particle in the unique unblocked odd site. Then, remove a particle from an even site at distance one from an antiknob, and finally add a particle in the unique unblocked odd site. Afterward, iterate the sequence of these two moves up to the target configuration $\eta \in \mathcal{C}_{ib}(\mathbf{e}, \mathbf{o})$. By construction, the resulting path has the desired property.

Let us now focus on case (ii). Consider the path described in Lemma 4.8(i) until it visits for the first time a configuration in $\mathcal{C}_{ir}(\mathbf{e}, \mathbf{o})$. Starting from such a configuration, add a particle in the

antiknob, obtaining a configuration η' that displays a unique non-degenerate odd cluster, which is a rhombus $\mathcal{R}_{\frac{L}{2}-1, \frac{L}{2}-1}$ with a single protuberance. Starting from η' , consider the path returned filling algorithm $\bar{\omega}$ up to the configuration $\eta \in \mathcal{C}_{gr}(\mathbf{e}, \mathbf{o})$. The described path has the desired property thanks to Proposition 3.4.

Consider now the concatenation of the paths described in Lemma 4.8(ii) and Lemma 4.9(i) until it visits for the first time a configuration in $\mathcal{C}_{ib}(\mathbf{e}, \mathbf{o})$. Starting from such a configuration, by iterating the pair of moves consisting of adding a particle to the unique unblocked odd site and removing a particle at distance one from an antiknob, it is possible to obtain a configuration with a unique non-degenerate cluster that contains $\mathcal{R}_{\frac{L}{2}-1, \frac{L}{2}-1}$. By construction, this resulting configuration is in $\mathcal{C}_{gr}(\mathbf{e}, \mathbf{o})$ and it is possible to iterate this couple of moves up to η . By construction, the resulting path has the desired property.

Consider now case (iii). Take the path described in Lemma 4.8(ii) until it visits for the first time the configuration in $\mathcal{C}_{sb}(\mathbf{e}, \mathbf{o})$ as in Figure 3 on the right. Starting from such a configuration, add a particle in the unique unblocked odd site. Then, remove a particle from an even site at distance one from an antiknob, and finally add a particle in the unique unblocked odd site. This configuration is in $\mathcal{C}_{mb}(\mathbf{e}, \mathbf{o})$. Afterward, iterate the sequence of these two moves up to the target configuration η . By construction, the resulting path has the desired property.

Consider now the concatenation of the paths described in Lemma 4.8(ii) and Lemma 4.9(i) until it visits for the first time a configuration in $\mathcal{C}_{ib}(\mathbf{e}, \mathbf{o})$. Starting from such a configuration, with the same procedure described above, it is possible to reach the target configuration $\eta \in \mathcal{C}_{mb}(\mathbf{e}, \mathbf{o})$ by visiting only saddles in $\mathcal{C}_{ib}(\mathbf{e}, \mathbf{o}) \cup \mathcal{C}_{mb}(\mathbf{e}, \mathbf{o})$.

Let us now focus on case (iv). Consider the concatenation of the paths described in Lemma 4.8(i) and Lemma 4.9(ii) until it visits for the first time a configuration in $\mathcal{C}_{gr}(\mathbf{e}, \mathbf{o})$. Starting from such a configuration, add a particle in the antiknob, obtaining a configuration η' . Note that η' is composed of a unique non-degenerate odd cluster, which is a rhombus $\mathcal{R}_{\frac{L}{2}-1, \frac{L}{2}-1}$ with a single protuberance. Starting from η' , consider the path returned by filling algorithm $\bar{\omega}$ up to the configuration $\eta \in \mathcal{C}_{cr}(\mathbf{e}, \mathbf{o})$. The described path has the desired property thanks to Proposition 3.4.

Consider now the concatenation of the paths described in Lemma 4.8(ii) and Lemma 4.9(iii) until it visits for the first time a configuration in $\mathcal{C}_{mb}(\mathbf{e}, \mathbf{o})$. Starting from such a configuration, by iterating the pair of moves consisting of adding a particle in the unique unblocked odd site and removing a particle at distance one from an antiknob, it is possible to obtain a configuration with a unique non-degenerate cluster that contains $\mathcal{R}_{\frac{L}{2}-1, \frac{L}{2}}$. By construction, this resulting configuration is in $\mathcal{C}_{cr}(\mathbf{e}, \mathbf{o})$ and it is possible to iterate this couple of moves up to η . By construction, the resulting path has the desired property. \square

Proof of Lemma 4.10. We start by proving (i). Arguing as in the proof of Lemma 4.9(ii) we can show that there exists a path with the desired property that connects η to $\bar{\eta} \in \mathcal{C}_{cr}(\mathbf{e}, \mathbf{o})$, where the unique non-degenerate cluster of $\bar{\eta}$ is $\mathcal{R}_{\frac{L}{2}-1, \frac{L}{2}}$ with attached a bar of length $\frac{L}{2} - 2$ and there is a degenerate rhombus $\mathcal{R}_{0,0}$ at distance one from an antiknob. Since the configuration displays two antiknobs, it is possible to sequentially add two particles in odd sites. Thus, by proceeding in this way the path reaches \mathbf{o} without visiting any other saddle and so the described path has the desired property.

Finally, consider case (ii). By arguing as in the proof of Lemma 4.9(iii)–(iv) we can show that there exists a path with the desired property that connects η to $\bar{\eta} \in \mathcal{C}_{gr}(\mathbf{e}, \mathbf{o}) \cup \mathcal{C}_{mb}(\mathbf{e}, \mathbf{o})$. If $\bar{\eta} \in \mathcal{C}_{gr}(\mathbf{e}, \mathbf{o})$, the claim follows by the previous argument. Otherwise, the configuration $\bar{\eta}$ has two antiknobs after arguing as above. In either case, the described path has the desired property. \square

Proof of Lemma 4.11. Consider first case (i). By construction, every non-backtracking optimal path from \mathbf{e} to \mathbf{o} that crosses a configuration in $\mathcal{C}_{ir}(\mathbf{e}, \mathbf{o})$ has to visit a configuration in $\mathcal{C}_{gr}(\mathbf{e}, \mathbf{o})$.

Indeed, each move consists in adding a particle in an unblocked odd site or removing a particle from an even site. Thus, it remains to consider backtracking optimal paths only. In order to visit a saddle in $\mathcal{C}_{ib}(\mathbf{e}, \mathbf{o})$, a column (or row) with precisely $\frac{L}{2} - 1$ particles arranged in odd sites needs to be created along these paths. To proceed, since we are considering backtracking optimal paths, the unique possibility is to visit a configuration in $\mathcal{C}_{sb}(\mathbf{e}, \mathbf{o})$ before reaching $\mathcal{C}_{ib}(\mathbf{e}, \mathbf{o})$. Thus, case (i) is concluded.

Consider now case (ii). The claim follows after noting that every configuration in $\mathcal{C}_{cr}(\mathbf{e}, \mathbf{o})$ contains one odd vertical (resp. horizontal) bridge B , where the two neighbouring columns (resp. rows) to B contains $\frac{L}{2} - 1$ odd particles each. Thus, all configurations in $\mathcal{C}_{cr}(\mathbf{e}, \mathbf{o})$ differ from a configuration in $\mathcal{C}_{ib}(\mathbf{e}, \mathbf{o})$ in at least two odd sites. Then, suppose that $\eta \in \mathcal{C}_{ib}(\mathbf{e}, \mathbf{o})$ and $\eta' \in \mathcal{C}_{cr}(\mathbf{e}, \mathbf{o})$ such that they differ in only two odd sites. Starting from η , if a bridge is created, then the resulting configuration is in $\mathcal{C}_{mb}(\mathbf{e}, \mathbf{o})$, while if the resulting configuration contains two neighbouring columns (or rows) with exactly $\frac{L}{2} - 1$ particles in odd sites, then it belongs to $\mathcal{C}_{gr}(\mathbf{e}, \mathbf{o})$. If the two configurations differ in at least three sites, we argue as above.

Consider now case (iii). The claim follows after arguing as in case (i) and noting that, in order to create a bridge, the path has to visit the set $\mathcal{C}_{sb}(\mathbf{e}, \mathbf{o})$. Lastly, in case (iv), the claim follows after arguing as in case (iii). □

5.3 Results on the saddles lying in the manifold \mathcal{V}_m^*

Proof of Lemma 4.13. We analyse separately the three cases.

Case (i). Suppose by contradiction that there exists a non-backtracking path $\omega' \in (\mathbf{e} \rightarrow \mathbf{o})_{\text{opt}}$ that crosses $\sigma \in \mathcal{V}_m^* \setminus \mathcal{C}_{ir}(\mathbf{e}, \mathbf{o})$ such that $R(\mathcal{O}^{nd}(\sigma))$ and $R(\mathcal{O}(\sigma))$ do not wind around the torus. First, since $\sigma \in \mathcal{V}_m^*$ and $\Delta H(\sigma) \leq L + 1$, we get

$$\begin{cases} e(\sigma) & \geq \frac{L^2}{4} - \frac{3}{2}, \\ o(\sigma) & \geq \frac{L^2}{4} - L + \frac{3}{2}. \end{cases} \tag{5.3}$$

Since $o(\sigma) > 0$ for any L , we deduce that σ cannot contain only degenerate clusters and therefore contains at least an odd non-degenerate cluster. Thus, one of the following cases occurs:

- (1) $\mathcal{O}(\sigma)$ consists of at least two non-degenerate odd clusters;
- (2) $\mathcal{O}(\sigma)$ consists of a single non-degenerate odd cluster different from $\mathcal{R}_{\frac{L}{2}-1, \frac{L}{2}-1}$ and possibly some degenerate clusters;
- (3) $\mathcal{O}(\sigma)$ consists of a single non-degenerate odd rhombus equal to $\mathcal{R}_{\frac{L}{2}-1, \frac{L}{2}-1}$ and at least one degenerate odd cluster $\mathcal{R}_{0,0}$ at distance greater than one from the non-degenerate one.

We consider the rhombus surrounding the odd non-degenerate region for all the above cases. Due to the isoperimetric inequality of Lemma 3.8, this rhombus \mathcal{R} has a perimeter $P(\mathcal{R})$ greater than or equal to $P(\mathcal{R}_{\frac{L}{2}-1, \frac{L}{2}-1})$, i.e., $P(\mathcal{R}) \geq 4(L - 1)$. In particular, for cases (1) and (2) we have $P(\mathcal{R}) > 4(L - 1)$ since $\mathcal{O}(\sigma) \neq \mathcal{R}_{\frac{L}{2}-1, \frac{L}{2}-1}$, and for case (3) we have $P(\mathcal{R}) = 4(L - 1)$. Let P_i denote the perimeter of the i -th cluster, with $i = 1, \dots, k$. Note that $P(\sigma) = \sum_{i=1}^k P_i$. We let $k_d \geq 0$ (resp. $k_{nd} \geq 1$) the number of degenerate clusters $\mathcal{R}_{0,0}$ (resp. non-degenerate clusters) such that the total number of clusters is $k = k_d + k_{nd} \geq 1$.

Subcase (1). In this case $k_{nd} \geq 2$, so that $k \geq 2$. Denote by \tilde{e}_i (resp. o_i) the number of empty even sites (resp. occupied odd sites) of the i -th cluster. Using (3.3), (3.7) and (3.8), we obtain

$$\begin{aligned} \Delta H(\sigma) &= \sum_{i=1}^k (\tilde{e}_i - o_i) = \sum_{i=1}^{k_d} \tilde{e}_i + \sum_{i=1}^{k_{nd}} (\tilde{e}_i - o_i) \geq \tilde{e}_d + \left(\sum_{i=1}^{k_{nd}} \tilde{e}_i + 2(k_{nd} - 1) - \sum_{i=1}^{k_{nd}} o_i \right) \\ &= \tilde{e}_d + \left(\sum_{i=1}^{k_{nd}} \tilde{e}_i - \sum_{i=1}^{k_{nd}} o_i \right) + 2(k_{nd} - 1) > \tilde{e}_d + (L - 1) + 2(k_{nd} - 1) \\ &\geq \tilde{e}_d + L + 1, \end{aligned} \tag{5.4}$$

where $\tilde{e}_d = \sum_{i=1}^{k_d} \tilde{e}_i$, the first inequality follows from the fact that the difference between the perimeter of two disjoint non-degenerate clusters and that of the cluster obtained by attaching the two is at least two, and the last inequality follows from the isoperimetric inequality applied to the cluster obtained by attaching the k clusters forming σ . Then, from inequalities (5.4) and $\Delta H(\sigma) \leq L + 1$, it follows that $\tilde{e}_d < 0$, which is a contradiction since $\tilde{e}_d \geq 0$.

Subcase (2). The unique non-degenerate odd cluster of σ has a shape different from a rhombus $\mathcal{R}_{\frac{1}{2}-1, \frac{1}{2}-1}$ by assumption. In this case $k_{nd} = 1$ and $k_d \geq 0$, so that $k = k_d + 1$. Thus, we obtain

$$\Delta H(\sigma) = \sum_{i=1}^{k_d+1} (\tilde{e}_i - o_i) = \sum_{i=1}^{k_d} \tilde{e}_i + (\tilde{e}_{k_d+1} - o_{k_d+1}) > \tilde{e}_d + L - 1, \tag{5.5}$$

where $\tilde{e}_d = \sum_{i=1}^{k_d} \tilde{e}_i$, the first equality follows from the fact that σ contains only one non-degenerate odd cluster, and the last inequality follows from the isoperimetric inequality applied to the non-degenerate cluster. Then by (5.5) and the fact that $\Delta H(\sigma) \leq L + 1$, we find $\tilde{e}_d \leq 1$ and so $k_d \leq 1$.

The configuration σ thus falls in one of the following three subcases:

- (2a) the only non-degenerate odd cluster of σ is a rhombus $\mathcal{R}_{\ell_1, \ell_2} \neq \mathcal{R}_{\frac{1}{2}-1, \frac{1}{2}-1}$;
- (2b) the non-degenerate odd cluster of σ is a cluster with $m \geq 1$ empty odd sites corresponding to some broken diagonal and $q = 0$ shorter diagonals;
- (2c) the non-degenerate odd cluster of σ is a cluster with $m \geq 0$ empty odd sites corresponding to some broken diagonal and $q \geq 1$ shorter diagonals.

We can ignore the case $m = 0$ and $q = 0$ as it corresponds to the rhombus $\mathcal{R}_{\frac{1}{2}-1, \frac{1}{2}-1}$.

Subcase (2a). This case is not admissible since, if $\mathcal{R}_{\ell_1, \ell_2} \neq \mathcal{R}_{\frac{1}{2}-1, \frac{1}{2}-1}$, we have

$$\begin{cases} \ell_1 + \ell_2 + 1 + k_d &= L + 1, \\ \ell_1 + \ell_2 + 1 &> L - 1, \end{cases}$$

and this implies $k_d > 2$, which is in contradiction with the assumption $k_d \leq 1$.

Subcase (2b). From the assumptions on σ , it follows that

$$\begin{cases} \ell_1 + \ell_2 + 1 + k_d + m &= L + 1, \\ \ell_1 + \ell_2 + 1 &> L - 1. \end{cases} \tag{5.6}$$

These give $k_d + m < 2$, which, in view of the inequalities $k_d \leq 1$ and $m \geq 1$, then imply that $k_d = 0$ and $m = 1$. Thus, we deduce that

$$\begin{cases} o(\sigma) &= \ell_1 \ell_2 - 1, \\ e(\sigma) &= (\ell_1 + 1)(\ell_2 + 1), \end{cases}$$

so that $\ell_1 + \ell_2 = L - 5$ since $\sigma \in \mathcal{V}_{m^*}$, but this contradicts the condition $\ell_1 + \ell_2 + 1 + k_d + m = L + 1$ in (5.6).

Subcase (2c). From the assumptions on σ , it follows that

$$\begin{cases} \ell_1 + \ell_2 + 1 + k_d + m = L + 1, \\ 2(\ell_1 + \ell_2 + 1) - q > 2(L - 1). \end{cases} \tag{5.7}$$

This implies that $2(k_d + m) + q \leq 3$, so we distinguish three subcases: **(2c-I)** $k_d = m = 0$ and $q \in \{1, 2, 3\}$; **(2c-II)** $k_d = 1, m = 0$ and $q = 1$; and **(2c-III)** $k_d = 0, m = 1$ and $q = 1$. The other subcases are not possible in view of the conditions $k_d \leq 1, m \geq 0$, and $q \geq 1$.

For subcase (2c-I), $k_d = m = 0$ and $q \in \{1, 2, 3\}$. Thus, by letting s be the total number of empty sites needed to be filled in order for the shorter diagonals to become complete, we deduce that

$$\begin{cases} o(\sigma) = \ell_1 \ell_2 - s, \\ e(\sigma) = (\ell_1 + 1)(\ell_2 + 1) - s, \end{cases}$$

so that $\ell_1 + \ell_2 = L - 4$ since $\sigma \in \mathcal{V}_{m^*}$, but this contradicts identity $\ell_1 + \ell_2 + 1 + k_d + m = L + 1$ in (5.7). The claims for (2c-II) and (2c-III) follow by arguing as in case (2c-I).

Subcase (3). First, note that $k_d \leq 2$, otherwise $\Delta H(\sigma) > L + 1$ and therefore the path ω would not be optimal.

If $k_d = 2$, using the non-backtracking property of the path ω , it follows that there is no possible move to cross the next manifold towards \mathbf{o} along an optimal path.

If $k_d = 1$, then $\Delta H(\sigma) = L$ so that the energy along the path can increase by at most 1 to reach \mathbf{o} . The unique possible move is to remove a particle from an empty site, obtaining a configuration with $k_d = 2$. We can then prove the claim by arguing as in case $k_d = 2$.

Case (ii). Suppose by contradiction that there exists a non-backtracking path $\omega' \in (\mathbf{e} \rightarrow \mathbf{o})_{\text{opt}}$ that crosses that crosses $\sigma \in \mathcal{V}_{m^*} \setminus \mathcal{C}_{ib}(\mathbf{e}, \mathbf{o})$ such that $R(\mathcal{O}^{nd}(\sigma))$ does not wind around the torus and $R(\mathcal{O}(\sigma))$ does. We observe that (5.3) holds for the configuration σ and, therefore, it contains at least one odd non-degenerate cluster and it cannot contain only degenerate clusters. Thus, we consider the following subcases:

- (1) $\mathcal{O}(\sigma)$ consists of at least two non-degenerate odd clusters;
- (2) $\mathcal{O}(\sigma)$ consists of a single non-degenerate odd cluster different from $\mathcal{R}_{\frac{L}{2}-1, \frac{L}{2}-1}$ and possibly some degenerate clusters;
- (3) $\mathcal{O}(\sigma)$ consists of a single non-degenerate odd rhombus equal to $\mathcal{R}_{\frac{L}{2}-1, \frac{L}{2}-1}$ and at least one degenerate odd cluster $\mathcal{R}_{0,0}$ at distance greater than one from the non-degenerate one.

Subcase (1). Suppose that σ contains $k \geq 2$ non-degenerate clusters $C_1(\sigma), \dots, C_k(\sigma)$. By assumption, all the rhombi surrounding $C_i(\sigma)$ do not wind around the torus for any $i = 1, \dots, k$; thus, we can argue as in case **(i-2c-II)** above.

Subcase (2). By arguing as in case **(i-2)** above, we deduce that this case is possible only when $\mathcal{R}(\mathcal{O}^{nd}(\sigma))$ does not wind around the torus and $\mathcal{R}(\mathcal{O}(\sigma))$ does, so that from (5.3) we deduce that there exists only one column or row with less than $L/2$ particles, but this contradicts the fact that $\sigma \notin \mathcal{C}_{ib}(\mathbf{e}, \mathbf{o})$.

Subcase (3). By arguing as in case **(i-3)** above, we deduce that this case is not possible.

Case (iii). Suppose by contradiction that there exists a non-backtracking path $\omega' \in (\mathbf{e} \rightarrow \mathbf{o})_{\text{opt}}$ that crosses that crosses $\sigma \in \mathcal{V}_{m^*} \setminus \mathcal{C}_{mb}(\mathbf{e}, \mathbf{o})$ such that both $R(\mathcal{O}^{nd}(\sigma))$ and $R(\mathcal{O}(\sigma))$ wind around the torus. We observe that (5.3) holds for the configuration σ , and therefore, it contains at least one odd non-degenerate cluster, and it cannot contain only degenerate clusters. Thus, we consider the following subcases:

- (1) $\mathcal{O}(\sigma)$ consists of at least two non-degenerate odd clusters;
- (2) $\mathcal{O}(\sigma)$ consists of a single non-degenerate odd cluster different from $\mathcal{R}_{\frac{L}{2}-1, \frac{L}{2}-1}$ and possibly some degenerate clusters;
- (3) $\mathcal{O}(\sigma)$ consists of a single non-degenerate odd rhombus equal to $\mathcal{R}_{\frac{L}{2}-1, \frac{L}{2}-1}$ and at least one degenerate odd cluster $\mathcal{R}_{0,0}$ at distance greater than one from the non-degenerate one.

Subcase (1). Suppose that σ contains $k \geq 2$ non-degenerate clusters $C_1(\sigma), \dots, C_k(\sigma)$. If the rhombus surrounding $C_i(\sigma)$ does not wind around the torus for any $i = 1, \dots, k$, we can argue as in case (i-1) above. Otherwise, suppose that there exists an index i such that $\mathcal{R}(C_i(\sigma))$ winds around the torus. Thus, there exists at least one row or column that contains $\frac{L}{2}$ particles, say a column. Since $k \geq 2$, this implies that there exists a row containing two odd particles that belong to $C_i(\sigma)$ and another disjoint cluster. Thus, the energy difference contribution ΔH along this row or column is at least two. In addition, all the other L rows or columns composing $C_i(\sigma)$ have an energy contribution of at least one. Thus, the total contribution is $\Delta H(\sigma) > 2 + L - 1 = L + 1$, where the strict inequality follows from $k \geq 2$. This contradicts the assumption $\Delta H(\sigma) \leq L + 1$, and therefore, this case is not admissible.

Subcase (2). By arguing as in case (i-2) above, we deduce that this case is possible only when both $\mathcal{R}(\mathcal{O}^{nd}(\sigma))$ and $\mathcal{R}(\mathcal{O}(\sigma))$ wind around the torus, so that from (5.3) we deduce that there exists at least one column or row with strictly less than $L/2$ particles, but this contradicts the fact that $\sigma \notin \mathcal{C}_{mb}(\mathbf{e}, \mathbf{o})$.

Subcase (3). By arguing as in case (i-3) above, we deduce that this case is not possible. □

6. Conclusions and future work

This work concludes the analysis of the low-temperature behaviour for the hard-core model on a square grid graph with periodic boundary conditions initiated by [47]. In that paper, this interacting particle system was shown to have two stable states, and the energy barrier between them was already identified. However, the argument carried out in that paper did not provide any geometrical insight into the trajectories followed by the process in the low-temperature limit and did not characterize the critical configurations, i.e., the states with the highest energy in these limiting trajectories. The goal of this paper was precisely to fill this gap. More precisely, we provide a geometrical description of all the essential saddles for this transition and highlight how these communicate with each other without exceeding the critical energy barrier $\Gamma(\Lambda)$.

The extension to other types of lattices naturally arises in this context. Indeed, in [56], the authors investigate the same model on the triangular lattice, studying the asymptotic behaviour of the hitting times between stable states but without providing any information on the critical configurations. The type of analysis carried out in this paper could be useful to tackle that problem, even if it looks more challenging since there are three stable states and isoperimetric inequalities are probably harder to derive. This will be the focus of future work. Another possible direction could be the study of the asymptotic behaviour of the hard-core model on square grid graphs but with different boundary conditions or in the presence of some impurities. However, in this case, we expect the transition between two stable states to most likely occur by heterogeneous nucleation starting from the boundary, hence breaking the intrinsic symmetry and translation-invariance properties of the critical configurations. On the other hand, we expect that the techniques and machinery developed in this paper will also be useful in identifying critical configurations of other interacting particle systems on finite square lattices with similar blocking effects, e.g., the Widom-Rowlinson model [55].

Acknowledgements

S.B and V.J. are grateful for the support of ‘Gruppo Nazionale per l’Analisi Matematica, la Probabilità e le loro Applicazioni’ (GNAMPA-INdAM). The authors are grateful to Francesca Nardi, Julien Sohler, Gianmarco Bet, and Tommaso Monni for useful and fruitful discussions at the early stage of this work.

References

- [1] Apollonio, V., Jacquier, V., Nardi, F. R. and Troiani, A. (2022) Metastability for the Ising model on the hexagonal lattice. *Electron J. Probab.* **27** 1–48. doi: [10.1214/22-ejp763](https://doi.org/10.1214/22-ejp763)
- [2] Baldassarri, S., Gallo, A., Jacquier, V. and Zocca, A. (2023) Ising model on clustered networks: A model for opinion dynamics. *Physica A: Stat. Mech. Appl.* **623** 128811. doi: [10.1016/j.physa.2023.128811](https://doi.org/10.1016/j.physa.2023.128811).
- [3] Baldassarri, S., Gaudillière, A., den Hollander, F., Nardi, F. R., Olivieri, E. and Scoppola, E. (2024) Droplet dynamics in a two-dimensional rarefied gas under Kawasaki dynamics. *Stoch. Proc. Appl.* **177** 104460. doi: [10.1016/j.spa.2024.104460](https://doi.org/10.1016/j.spa.2024.104460).
- [4] Baldassarri, S. and Jacquier, V. (2023) Metastability for Kawasaki dynamics on the hexagonal lattice. *J. Stat. Phys.* **190** 1–44. doi: [10.1007/s10955-022-03061-8](https://doi.org/10.1007/s10955-022-03061-8)
- [5] Baldassarri, S. and Nardi, F. R. (2022) Critical droplets and sharp asymptotics for Kawasaki dynamics with strongly anisotropic interactions. *J. Stat. Phys.* **186** 1–46. doi: [10.1007/s10955-022-02874-x](https://doi.org/10.1007/s10955-022-02874-x)
- [6] Baldassarri, S. and Nardi, F. R. (2022) Critical droplets and sharp asymptotics for Kawasaki dynamics with weakly anisotropic interactions. *Stoch. Proc. Appl.* **147** 107–144. doi: [10.1016/j.spa.2022.01.011](https://doi.org/10.1016/j.spa.2022.01.011).
- [7] Baldassarri, S. and Nardi, F. R. (2021) Metastability in a lattice gas with strong anisotropic interactions under Kawasaki dynamics. *Electron J. Probab.* **26** 1–66. doi: [10.1214/21-ejp701](https://doi.org/10.1214/21-ejp701)
- [8] Beltrán, J. and Landim, C. (2014) A Martingale approach to metastability. *Probability Theory and Related Fields* **161** 267–307. doi: [10.1007/s00440-014-0549-9](https://doi.org/10.1007/s00440-014-0549-9).
- [9] Beltrán, J. and Landim, C. (2010) Tunneling and metastability of continuous time Markov chains. *J. Stat. Phys.* **140** 1065–1114. doi: [10.1007/s10955-010-0030-9](https://doi.org/10.1007/s10955-010-0030-9).
- [10] van den Berg, J. and Steif, J. E. (1994) Percolation and the hard-core lattice gas model. *Stoch. Proc. Appl.* **49** 179–197. doi: [10.1016/0304-4149\(94\)90132-5](https://doi.org/10.1016/0304-4149(94)90132-5).
- [11] Bet, G., Gallo, A. and Kim, S. (2023) Metastability of the three-state Potts model with general interactions. *Electron J. Probab.* **28** 1–37. doi: [10.1214/23-EJP1003](https://doi.org/10.1214/23-EJP1003)
- [12] Bet, G., Gallo, A. and Nardi, F. R. (2021) Critical configurations and tube of typical trajectories for the Potts and Ising models with zero external field. *J. Stat. Phys.* **184** 1–38. doi: [10.1007/s10955-021-02814-1](https://doi.org/10.1007/s10955-021-02814-1)
- [13] Bet, G., Gallo, A. and Nardi, F. R. (2022) Metastability for the degenerate Potts model with negative external magnetic field under Glauber dynamics. *J. Math. Phys.* **63** 123303. doi: [10.1063/5.0099480](https://doi.org/10.1063/5.0099480).
- [14] Bet, G., Gallo, A. and Nardi, F. R. (2024) Metastability for the degenerate Potts Model with positive external magnetic field under Glauber dynamics. *Stoch. Proc. Appl.* **172** 104343. doi: [10.1016/j.spa.2024.104343](https://doi.org/10.1016/j.spa.2024.104343).
- [15] Bet, G., Jacquier, V. and Nardi, F. R. (2021) Effect of energy degeneracy on the transition time for a series of metastable states. *J. Stat. Phys.* **184** 1–42. doi: [10.1007/s10955-021-02788-0](https://doi.org/10.1007/s10955-021-02788-0)
- [16] Bianchi, A., Gaudillière, A. and Milanese, P. (2020) On Soft Capacities, Quasi-stationary Distributions and the pathwise approach to metastability. *J. Stat. Phys.* **181** 1052–1086. doi: [10.1007/s10955-020-02618-9](https://doi.org/10.1007/s10955-020-02618-9).
- [17] Bianchi, A. and Gaudillière, A. (2016) Metastable states, quasi-stationary distributions and soft measures. *Stoch. Proc. Appl.* **126** 1622–1680. doi: [10.1016/j.spa.2015.11.015](https://doi.org/10.1016/j.spa.2015.11.015).
- [18] Blanca, A., Chen, Y., Galvin, D., Randall, D. and Tetali, P. (2019) Phase coexistence for the hard-core model on $\text{mathbb{Z}}^2$. *Comb. Probab. Comput.* **28** 1–22. doi: [10.1017/s0963548318000238](https://doi.org/10.1017/s0963548318000238).
- [19] Borgs, C., Chayes, J., Frieze, A., Kim, J. H., Tetali, P., Vigoda, E. and Vu, V. H. (1999) Torpid mixing of some Monte Carlo Markov chain algorithms in statistical physics, 40th Annual Symposium on Foundations of Computer Science (Cat. No.99CB37039), 218–229. doi: [10.1109/sffcs.1999.814594](https://doi.org/10.1109/sffcs.1999.814594)
- [20] Bovier, A., den Hollander, F. and Nardi, F. (2005) Sharp asymptotics for Kawasaki dynamics on a finite box with open boundary. *Probab. Theory Rel.* **135** 265–310. doi: [10.1007/s00440-005-0460-5](https://doi.org/10.1007/s00440-005-0460-5).
- [21] Bovier, A., den Hollander, F. and Spitoni, C. (2010) Homogeneous nucleation for Glauber and Kawasaki dynamics in large volumes at low temperatures. *Ann. Probab.* **38** 661–713. doi: [10.1214/09-AOP492](https://doi.org/10.1214/09-AOP492).
- [22] Bovier, A., Eckhoff, M., Gaynard, V. and Klein, M. (2002) Metastability and low lying spectra in reversible Markov Chains. *Commun. Math. Phys.* **228** 219–255. doi: [10.1007/s002200200609](https://doi.org/10.1007/s002200200609).
- [23] Bovier, A. and den Hollander, F. (2015) *Metastability*. Springer International Publishing. doi: [10.1007/978-3-319-24777-9](https://doi.org/10.1007/978-3-319-24777-9)
- [24] Cassandro, M., Galves, A., Olivieri, E. and Vares, M. E. (1984) Metastable behavior of stochastic dynamics: A pathwise approach. *J. Stat. Phys.* **35** 603–634. doi: [10.1007/bf01010826](https://doi.org/10.1007/bf01010826).
- [25] Cirillo, E. N. M., Jacquier, V. and Spitoni, C. (2024) Homogeneous and heterogeneous nucleation in the three-state Blume-Capel model. *Phys. D: Nonlinear Phenom.* **461** 134125. doi: [10.1016/j.physd.2024.134125](https://doi.org/10.1016/j.physd.2024.134125).

- [26] Cirillo, E. N. M. and Nardi, F. R. (2013) Relaxation height in energy landscapes: An application to multiple metastable states. *J. Stat. Phys.* **150** 1080–1114. doi: [10.1007/s10955-013-0717-9](https://doi.org/10.1007/s10955-013-0717-9).
- [27] Cirillo, E. N. M., Nardi, F. R. and Sohler, J. (2015) Metastability for general dynamics with rare transitions: Escape time and critical configurations. *J. Stat. Phys.* **161** 365–403. doi: [10.1007/s10955-015-1334-6](https://doi.org/10.1007/s10955-015-1334-6).
- [28] Cirillo, E. N. M., Nardi, F. R. and Spitoni, C. (2008) Competitive nucleation in reversible probabilistic cellular automata. *Phys. Rev. E* **78** 1–4. doi: [10.1103/physreve.78.040601](https://doi.org/10.1103/physreve.78.040601).
- [29] Cirillo, E. N. M., Nardi, F. R. and Spitoni, C. (2008) Metastability for reversible probabilistic cellular automata with self-interaction. *J. Stat. Phys.* **132** 431–471. doi: [10.1007/s10955-008-9563-6](https://doi.org/10.1007/s10955-008-9563-6).
- [30] Cirillo, E. N. M., Jacquier, V. and Spitoni, C. (2022) Metastability of synchronous and asynchronous dynamics. *Entropy* **24** 450. doi: [10.3390/e24040450](https://doi.org/10.3390/e24040450).
- [31] Galvin, D. (2008) Sampling independent sets in the discrete torus. *Random Struct. Algor.* **33** 356–376. doi: [10.1002/rsa.20223](https://doi.org/10.1002/rsa.20223).
- [32] Galvin, D. and Tetali, P. (2004) Slow mixing of Glauber dynamics for the hard-core model on the hypercube. In Proceedings of the 15th annual ACM-SIAM Symposium on Discrete Algorithms, Vol. **11**, pp. 466–467.
- [33] Galvin, D. and Tetali, P. (2006) Slow mixing of Glauber dynamics for the hardcore model on regular bipartite graphs. *Random Struct Algor* **28** 427–443. doi: [10.1002/rsa.20094](https://doi.org/10.1002/rsa.20094).
- [34] Gaudillière, A., den Hollander, F., Nardi, F. R., Olivieri, E. and Scoppola, E. (2009) Ideal gas approximation for a two-dimensional rarefied gas under Kawasaki dynamics. *Stoch. Proc. Appl.* **119** 737–774. doi: [10.1016/j.spa.2008.04.008](https://doi.org/10.1016/j.spa.2008.04.008).
- [35] Gaunt, D. S. and Fisher, M. E. (1965) Hard-sphere lattice gases. I. Plane-square lattice. *The Journal of Chemical Physics* **43** 2840–2863. doi: [10.1063/1.1697217](https://doi.org/10.1063/1.1697217).
- [36] Greenberg, S. and Randall, D. (2010) Slow mixing of Markov chains using fault lines and fat contours. *Algorithmica* **58** 911–927. doi: [10.1007/s00453-008-9246-3](https://doi.org/10.1007/s00453-008-9246-3).
- [37] den Hollander, F., Olivieri, E. and Scoppola, E. (2000) Metastability and nucleation for conservative dynamics. *J. Math. Phys.* **41** 1424–1498. doi: [10.1063/1.533193](https://doi.org/10.1063/1.533193).
- [38] Jauslin, I. and Lebowitz, J. L. (2018) High-fugacity expansion, Lee-Yang Zeros, and Order-Disorder Transitions in hard-core lattice Systems. *Commun. Math. Phys.* **364** 655–682. doi: [10.1007/s00220-018-3269-7](https://doi.org/10.1007/s00220-018-3269-7), eprint: 1708.01912.
- [39] Kahn, J. (2001) An entropy approach to the hard-core model on bipartite graphs. *Comb. Probab. Comput.* **10** 219–237. doi: [10.1017/s0963548301004631](https://doi.org/10.1017/s0963548301004631).
- [40] Kim, S. and Seo, I. (2022) Approximation method to metastability: An application to non-reversible, two-dimensional Ising and Potts models without external fields, to appear in *Annals of Probability*.
- [41] Landim, C., Marcondes, D. and Seo, I. (2023) A resolvent approach to metastability. *J Eur Math Soc* 1–56, published online first. doi: [10.4171/JEMS/1398](https://doi.org/10.4171/JEMS/1398)
- [42] Luby, M. and Vigoda, E. (1999) Fast convergence of the Glauber dynamics for sampling independent sets. *Random Struct. Algor.* **15** 229–241. doi: [10.1002/\(sici\)1098-2418\(199910/12\)15:3<417::aid-rsa3gt.3.0.co;2-x](https://doi.org/10.1002/(sici)1098-2418(199910/12)15:3<417::aid-rsa3gt.3.0.co;2-x).
- [43] Manzo, F., Nardi, F. R., Olivieri, E. and Scoppola, E. (2004) On the essential features of metastability: tunnelling time and critical configurations. *J. Stat. Phys.* **115** 591–642. doi: [10.1023/b:joss.0000019822.45867.ec](https://doi.org/10.1023/b:joss.0000019822.45867.ec).
- [44] Martinelli, F., Sinclair, A. and Weitz, D. (2007) Fast mixing for independent sets, colorings, and other models on trees. *Random Struct. Algor.* **31** 134–172. doi: [10.1002/rsa.20132](https://doi.org/10.1002/rsa.20132).
- [45] Mossel, E., Weitz, D. and Wormald, N. (2009) On the hardness of sampling independent sets beyond the tree threshold. *Probab. Theory Relat. Fields.* **143** 401–439. doi: [10.1007/s00440-007-0131-9](https://doi.org/10.1007/s00440-007-0131-9).
- [46] Nardi, F. R., Olivieri, E. and Scoppola, E. (2005) Anisotropy effects in nucleation for conservative dynamics. *J. Stat. Phys.* **119** 539–595. doi: [10.1007/s10955-004-3247-7](https://doi.org/10.1007/s10955-004-3247-7).
- [47] Nardi, F. R., Zocca, A. and Borst, S. C. (2015) Hitting time asymptotics for hard-core interactions on grids. *J. Stat. Phys.* **162** 522–576. doi: [10.1007/s10955-015-1391-x](https://doi.org/10.1007/s10955-015-1391-x).
- [48] Nardi, F. R. and Spitoni, C. (2012) Sharp asymptotics for stochastic dynamics with parallel updating rule. *J. Stat. Phys.* **146** 701–718. doi: [10.1007/s10955-011-0413-6](https://doi.org/10.1007/s10955-011-0413-6).
- [49] Nardi, F. R. and Zocca, A. (2019) Tunneling behavior of Ising and Potts models in the low-temperature regime. *Stoch. Proc. Appl.* **129** 4556–4575. doi: [10.1016/j.spa.2018.12.001](https://doi.org/10.1016/j.spa.2018.12.001).
- [50] Olivieri, E. and Scoppola, E. (1995) Markov chains with exponentially small transition probabilities: First exit problem from a general domain. I. The reversible case. *J. Stat. Phys.* **79** 613–647. doi: [10.1007/bf02184873](https://doi.org/10.1007/bf02184873).
- [51] Olivieri, E. and Scoppola, E. (1996) Markov chains with exponentially small transition probabilities: First exit problem from a general domain. II. The general case. *J. Stat. Phys.* **84** 987–1041. doi: [10.1007/bf02174126](https://doi.org/10.1007/bf02174126).
- [52] Olivieri, E. and Vares, M. E. (2005) *Large Deviations and Metastability*. Cambridge University Press, doi: [10.1017/cbo9780511543272](https://doi.org/10.1017/cbo9780511543272)
- [53] Randall, D. (2006) Slow mixing of Glauber dynamics via topological obstructions. In Proceedings of the seventeenth annual ACM-SIAM symposium on Discrete algorithm - SODA '06, pp. 870–879. doi: [10.1145/1109557.1109653](https://doi.org/10.1145/1109557.1109653).
- [54] Zocca, A. (2015) Spatio-temporal dynamics of random-access networks: An interacting particle approach” [PhD thesis]. Eindhoven University of Technology. ISBN: 978-90-386-3981-9
- [55] Zocca, A. (2018) Low-temperature behavior of the multicomponent widom-rowlison model on finite square lattices. *J. Stat. Phys.* **171** 1–37. doi: [10.1007/s10955-018-1961-9](https://doi.org/10.1007/s10955-018-1961-9).
- [56] Zocca, A. (2018) Tunneling of the hard-core model on finite triangular lattices. *Random Struct. Algor.* **55** 215–246. doi: [10.1002/rsa.20795](https://doi.org/10.1002/rsa.20795).

[57] Zocca, A., Borst, S. C., van Leeuwen, J. S. and Nardi, F. R. (2013) Delay performance in random-access grid networks. *Perform. Eval.* **70** 900–915. doi: [10.1016/j.peva.2013.08.019](https://doi.org/10.1016/j.peva.2013.08.019).

A. Appendix A

Proof of Lemma 3.1. We start by proving (i). Given $0 \leq k_1^* \leq \ell_1$ and $\ell_2 + 1 \leq j_1^* \leq L - 1$, we want to show that there exists $0 \leq k_2^* \leq \ell_1$ and $0 \leq j_2^* \leq \ell_2$ such that

$$\begin{cases} k_1^* + j_1^* = k_2^* + j_2^* \pmod{L}, \\ k_1^* - j_1^* = k_2^* - j_2^* \pmod{L}. \end{cases} \tag{A.1}$$

The choice $j_2^* = j_1^* + L/2 \pmod{L}$ and $k_2^* = k_1^* + L/2 \pmod{L}$ implies the claim in (i), since the chosen indices j_2^* and k_2^* satisfy (A.1) and they are modulo L such that

$$\begin{cases} j_2^* \geq \ell_2 + 1 + \frac{L}{2} \geq 1, \\ j_2^* \leq L - 1 + \frac{L}{2} \leq \ell_2 - 1, \\ k_2^* \geq \frac{L}{2}, \\ k_2^* \leq \ell_1 + \frac{L}{2} \leq \frac{L}{2} - 2 \leq \ell_1 - 2. \end{cases}$$

By interchanging the role of k_1^* and k_2^* and arguing in the same way, the proof of (i) is concluded. The two inclusions stated in (ii) can be proved by arguing in an analogous way. \square

Proof of Lemma 3.2. In this proof, all the sums will be tacitly assumed to be taken modulo L . Denote $\eta = (\eta_1, \eta_2) \in V_o$. We analyse each case separately.

Case (i). Considering $S_{\ell_1, \ell_2}(\eta) \subset V_o$ and $\partial^+ S_{\ell_1, \ell_2}(\eta) \subset V_e$, we observe that

$$\begin{aligned} V \setminus \mathcal{R}_{\ell_1, \ell_2}(\eta) &= V \setminus \{S_{\ell_1, \ell_2}(\eta) \cup \partial^+ S_{\ell_1, \ell_2}(\eta)\} \\ &= \{V_o \cup V_e\} \setminus \{S_{\ell_1, \ell_2}(\eta) \cup \partial^+ S_{\ell_1, \ell_2}(\eta)\} \\ &= \{V_o \setminus \{S_{\ell_1, \ell_2}(\eta) \cup \partial^+ S_{\ell_1, \ell_2}(\eta)\}\} \cup \{V_e \setminus \{S_{\ell_1, \ell_2}(\eta) \cup \partial^+ S_{\ell_1, \ell_2}(\eta)\}\} \\ &= \{V_o \setminus S_{\ell_1, \ell_2}(\eta)\} \cup \{V_e \setminus \partial^+ S_{\ell_1, \ell_2}(\eta)\}. \end{aligned} \tag{A.2}$$

Thus, we want to show that the two subsets are equal to $S_{\hat{i}_1, \hat{i}_2}(\hat{\eta})$ and $\partial^+ S_{\hat{i}_1, \hat{i}_2}(\hat{\eta})$ for some $0 \leq \hat{i}_1, \hat{i}_2 \leq L - 1$ and $\hat{\eta} \in V_e$. In addition, we may write

$$V_e = \bigcup_{0 \leq k', j' \leq L-1} \{(k' + j', k' - j')\} \tag{A.3}$$

and

$$\partial^+ S_{\ell_1, \ell_2}(\eta) = \bigcup_{\substack{0 \leq k \leq \ell_1 \\ 0 \leq j \leq \ell_2}} \{(\eta_1 + k + j - 1, \eta_2 + k - j)\}. \tag{A.4}$$

Thus, we have

$$\begin{aligned}
 V_e \setminus \partial^+ S_{\ell_1, \ell_2}(\eta) &= \bigcup_{0 \leq k', j' \leq L-1} \{(k' + j' + \eta_1 - 1, k' - j' + \eta_2)\} \setminus \bigcup_{\substack{0 \leq k \leq \ell_1 \\ 0 \leq j \leq \ell_2}} \{(\eta_1 + k + j - 1, \eta_2 + k - j)\} \\
 &= \bigcup_{\substack{\ell_1+1 \leq \tilde{k} \leq L-1 \\ \ell_2+1 \leq \tilde{j} \leq L-1}} \{(\tilde{k} + \tilde{j} + \eta_1 - 1, \tilde{k} - \tilde{j} + \eta_2)\} \\
 &= \bigcup_{\substack{0 \leq \hat{k} \leq L-\ell_1-2 \\ 0 \leq \hat{j} \leq L-\ell_2-2}} \{(\hat{k} + \hat{j} + \ell_1 + \ell_2 + 2 + \eta_1 - 1, \hat{k} - \hat{j} + \ell_1 - \ell_2 + \eta_2)\}, \tag{A.5}
 \end{aligned}$$

where at the second equality we used Lemma 3.1(i) and at the last equality we used the change of variables $\hat{k} = \tilde{k} - (\ell_1 + 1)$ and $\hat{j} = \tilde{j} - (\ell_2 + 1)$. Now, we consider $\hat{\eta} = (\ell_1 + \ell_2 + 1 + \eta_1, \ell_1 - \ell_2 + \eta_2) \in V_e$ and we obtain

$$V_e \setminus \partial^+ S_{\ell_1, \ell_2}(\eta) = \bigcup_{\substack{0 \leq \hat{k} \leq L-\ell_1-2 \\ 0 \leq \hat{j} \leq L-\ell_2-2}} \{(\hat{k} + \hat{j} + \hat{\eta}_1, \hat{k} - \hat{j} + \hat{\eta}_2)\} \tag{A.6}$$

Thus, we have $V_e \setminus \partial^+ S_{\ell_1, \ell_2}(\eta) = S_{L-\ell_1-1, L-\ell_2-1}(\hat{\eta}) \subseteq V_e$. Arguing as above, we prove that $V_o \setminus S_{\ell_1, \ell_2}(\eta) = \partial^+ S_{L-\ell_1-1, L-\ell_2-1}(\hat{\eta}) \subseteq V_o$.

Case (ii). Without loss of generality we may assume $\ell_1 = \min\{\ell_1, \ell_2\}$. For $\eta = (\eta_1, \eta_2) \in V_e$, by using (A.3) and (3.11), we have

$$\begin{aligned}
 V_e &= \bigcup_{\substack{0 \leq k \leq \ell_1 \\ 0 \leq j \leq L-1}} \{(k + j + \eta_1, k - j + \eta_2)\} \cup \bigcup_{\substack{\ell_1+1 \leq k \leq L-1 \\ 0 \leq j \leq L-1}} \{(k + j + \eta_1, k - j + \eta_2)\} \\
 &= \bigcup_{\substack{0 \leq k \leq \ell_1 \\ 0 \leq j \leq L-1}} \{(k + j + \eta_1, k - j + \eta_2)\} = \partial^+ S_{\ell_1, L-1}(\eta). \tag{A.7}
 \end{aligned}$$

Thus, it follows that all even sites belong to the rhombus $\mathcal{R}_{\ell_1, \ell_2}(\eta)$. In addition, by using (3.12) we obtain

$$\begin{aligned}
 S_{\ell_1, L-1}(\eta) &= \bigcup_{\substack{0 \leq k \leq \ell_1-1 \\ 0 \leq j \leq L-2}} \{(\eta_1 + k' + j', \eta_2 + k' - j')\} \\
 &= \bigcup_{\substack{0 \leq k \leq \frac{L}{2}-1 \\ 0 \leq j \leq L-2}} \{(\eta_1 + k + j, \eta_2 + k - j)\} \cup \bigcup_{\substack{\frac{L}{2} \leq k \leq \ell_1-1 \\ 0 \leq j \leq L-2}} \{(\hat{\eta}_1 + k + j, \hat{\eta}_2 + k - j)\} \\
 &= \bigcup_{\substack{0 \leq k \leq \frac{L}{2}-1 \\ 0 \leq j \leq L-2}} \{(\eta_1 + k + j, \eta_2 + k - j)\} \cup \bigcup_{L/2 \leq k \leq \ell_1-1} \{(\hat{\eta}_1 + k, \hat{\eta}_2 + k)\}. \tag{A.8}
 \end{aligned}$$

Thus, we deduce that the rhombus $\mathcal{R}_{\ell_1, L-1}(\eta)$ contains $L^2/2 - L + \ell_1$ odd sites, which implies that its complement in V contains $L - \ell_1$ odd sites.

Case (iii). Without loss of generality we may assume $\ell_1 = \min\{\ell_1, \ell_2\}$. In this case, after using the same argument we have shown above, for some $\hat{\eta} = (\hat{\eta}_1, \hat{\eta}_2) \in V_{\mathbf{o}}$ we obtain that

$$V_{\mathbf{o}} \setminus S_{\ell_1, L}(\eta) = \bigcup_{\substack{\ell_1 \leq k \leq \frac{L}{2} - 1 \\ 0 \leq j \leq L - 1}} \{(\hat{\eta}_1 + k + j, \hat{\eta}_2 + k - j)\} \tag{A.9}$$

and

$$V_{\mathbf{e}} \setminus \partial^+ S_{\ell_1, L}(\eta) = \bigcup_{\substack{\ell_1 + 1 \leq k \leq \frac{L}{2} - 1 \\ 0 \leq j \leq L - 1}} \{(\hat{\eta}_1 + k + j - 1, \hat{\eta}_2 + k - j)\}. \tag{A.10}$$

This implies that the rhombus $\mathcal{R}_{\ell_1, L}(\eta)$ contains $L \ell_1$ odd sites and $L(\ell_1 + 1)$ even sites.

Case (iv). By arguing as above, we can show that the complement of the rhombus $\mathcal{R}_{\ell_1, \ell_2}(\eta)$ in V has no even and odd sites and therefore $\mathcal{R}_{\ell_1, \ell_2} \equiv V$. □